

## Article

# Nodulating *Aeschynomene indica* without Nod Factor Synthesis Genes: In Silico Analysis of Evolutionary Relationship

Mengguang Zhao <sup>1,†</sup>, Jingyi Dong <sup>1,†</sup>, Zhenpeng Zhang <sup>2</sup>, Entao Wang <sup>3</sup>, Dandan Wang <sup>1</sup>, Huijie Xie <sup>1</sup>, Chao Wang <sup>1</sup> and Zhihong Xie <sup>1,\*</sup>

- <sup>1</sup> National Engineering Laboratory for Efficient Utilization of Soil and Fertilizer Resources, Shandong Engineering Research Center of Plant-Microbia Restoration for Saline-Alkali Land, College of Resources and Environment, Shandong Agricultural University, Taian 271000, China
- <sup>2</sup> Key Laboratory of Coastal Environmental Processes and Ecological Remediation, Yantai Institute of Coastal Zone Research, Chinese Academy of Sciences, Yantai 264003, China
- <sup>3</sup> Departamento de Microbiología, Escuela Nacional de Ciencias Biológicas, Instituto Politécnico Nacional, Mexico City 11350, Mexico
- \* Correspondence: zhihongxie211@163.com; Tel.: +86-183-5357-1476
- † These authors contributed equally to this work.

**Abstract:** *Aeschynomene indica* rhizobia (AIRs) are special classes of bacteria capable of nodulating without nodulation factors and have photosynthetic capacity. With an aim to characterize the structural variations in *Bradyrhizobium* genomes during its evolution, the genomes of AIRs and the reference *Bradyrhizobium* strains were compared utilizing molecular biology, bioinformatics, and biochemistry techniques. The presence of symbiotic nitrogen fixation (*nif*) genes and photosynthetic genes, as well as components of the T3SS (Type III secretion system) and T3CP (Type III chaperone) in the genome of AIRs, was also assessed. Additionally, the origin, evolutionary history, and genes associated with the NF-independent nodulation pattern in AIRs were explored. The results indicate that horizontal gene transfer events have occurred in AIRs, and three distinct origins of AIRs were estimated: early differentiated AIRs, non-symbiotic *Bradyrhizobium*, and non-AIRs. In contrast to the significant genetic transformations observed in the second and third groups, the first group of AIRs displays a rich evolutionary history, exhibits high species diversity, and primarily relies on vertical transmission of nitrogen fixation and photosynthetic genes. Overall, the findings provide a fundamental theoretical foundation for gaining a deeper understanding of the phylogeny and genealogy of AIRs.

**Keywords:** *Aeschynomene indica* rhizobia; phylogenetic analysis; photosynthesis gene cluster; nitrogen fixation gene cluster; evolution; comparative genome



**Citation:** Zhao, M.; Dong, J.; Zhang, Z.; Wang, E.; Wang, D.; Xie, H.; Wang, C.; Xie, Z. Nodulating *Aeschynomene indica* without Nod Factor Synthesis Genes: In Silico Analysis of Evolutionary Relationship. *Agronomy* **2024**, *14*, 1295. <https://doi.org/10.3390/agronomy14061295>

Academic Editor: John Stephen C. Smith

Received: 29 April 2024

Revised: 11 June 2024

Accepted: 12 June 2024

Published: 15 June 2024



**Copyright:** © 2024 by the authors. Licensee MDPI, Basel, Switzerland. This article is an open access article distributed under the terms and conditions of the Creative Commons Attribution (CC BY) license (<https://creativecommons.org/licenses/by/4.0/>).

## 1. Introduction

*Aeschynomene indica* L. is an annual herb or subshrub within the Leguminosae family that can form both stem and root nodules with rhizobia [1,2]. Based on their differences in nodulation patterns with *Bradyrhizobium*, *Aeschynomene* species can be classified into three cross-inoculation (CI) groups [3]: Group CI-I species represented by *A. elaphroxylon* can only form root nodules with non-photosynthetic and weakly specific *Bradyrhizobium* strains (like ORS301) [4]. This nodulation process relies on signal exchange between the rhizobia and the hosts. Species in CI-II, like *A. afraspera*, are capable of nodulating with non-photosynthetic strains (such as ORS354) on roots only and with photosynthetic strains (such as ORS285) on both roots and stems. And CI-III species, like *A. indica* and *A. sensitiva*, can nodulate on both roots and stems with photosynthetic strains (such as ORS278). Notably, some CI-II rhizobia have *Nod* genes and can produce tumorigenic factors, while no strain containing *Nod* genes has been found in CI-III rhizobia [1]. In association with *Aeschynomene* in these three CI groups, the symbiotic *Bradyrhizobium*

strains present differences in three aspects: nodulating on roots only or on both roots and stems, photosynthesis or non-photosynthesis, and with/without *nod* genes. Therefore, the *Aeschynomene*-nodulating bradyrhizobia should present great variations in chromosome structure or gene composition during their co-evolution with the host plants. A thorough comparative study of genomes of different types of *Aeschynomene*-nodulating bradyrhizobia might give information about how the rhizobia evolved to nodulate the diverse CI groups of *Aeschynomene* species.

The photosynthetic ability of *Aeschynomene*-nodulating bradyrhizobia was believed to be similar to that in cyanobacteria and a number of other bacterial groups [5], while all of the photosynthesis species in *Bradyrhizobium* have been classified into the photosynthetic supergroup [5,6], corresponding to the dominant symbionts (*B. oligotrophicum*, *B. denitrificans*, and *B. aeschynomenes*) of *Aeschynomene* species [5,7,8]. Previously, a complex evolutionary history of photosynthesis has been found in *Bradyrhizobium* strains [9], and *Bradyrhizobium* sp. BTAi1 was the first strain found to nodulate with *A. indica* and capable of photosynthesis [10–12], which has been studied as a model of photosynthetic bradyrhizobia. This photosynthetic pigment-dependent property of AIRs is similar to that of photoheterotrophs [13–15], such as in the purple bacteria of *Rhodospseudomonas*. In these bacteria, *bch* and *crt* genes encode bacterial chlorophylls and carotenoids, respectively, while *puf* genes encode components of light capture complexes (*pufA* and *pufB* genes) and reaction centers (*pufL* and *pufM* genes).

Researchers have identified five types of *puf* operons, differing mainly in the number and arrangement of genes. However, it is noteworthy to mention that *pufL* and *pufM* genes are consistently present in all five *puf* operons. Consequently, the *pufLM* gene is commonly used as a target gene for photosynthetic centers [16,17]. Subsequently, it was discovered that some rhizobia isolated from stem nodules of *A. indica* also possessed photosynthetic pigments. Notably, all AIR strains containing photosynthetic pigments were capable of forming stem nodules with *A. indica* [4]. Furthermore, mutations in the photosynthetic genes reduced the number of nodules by 50% and had a corresponding impact on *nif* activity and plant growth [16]. So, the photosynthetic ability is also linked to the procedure of symbiosis, but its mechanism is still not clear [9]. It could be expected that a comparison of the genomes between the photosynthetic and non-photosynthetic strains would offer some information about their evolutionary relationships, while the genes mentioned above might be valuable markers for this kind of study.

It is widely accepted that the initiation of symbiosis between legumes and rhizobia relies on nodulation factor (NF) signaling [18]; however, the absence of *nod* genes in the genomes of two photosynthetic *Bradyrhizobium* strains (BTAi1 and ORS278) has been demonstrated [19–21]. So, the photosynthetic *Bradyrhizobium* strains presented an NF-independent nodulation mode in which the type III secretion system (T3SS) played a crucial role in symbiosis [22–24]. Similar to that of the nodulation genes, activation of T3SS in rhizobia is triggered by flavonoids secreted by the plant root system [25,26]: when rhizobia sense signals such as flavonoids, the T3SS transcriptional regulator *TtsI* binds to the *tts* box locus within the T3SS promoter, initiating T3SS activation [27,28]. It has been reported that T3SS-encoding genes are also located in the symbiosis island, similar to the *nod* genes, which is able to disperse between species via horizontal gene transfer (HGT) [29]. Based on the information mentioned above, it could be estimated that *nod* gene loss and T3SS gene adaptation might have happened in the photosynthetic *Bradyrhizobium* since both the gene loss events and HGT are substantial for genome alterations in bacteria [30,31]. Moreover, it is indispensable to gain symbiotic genes through HGT [32].

AIRs are a unique group of rhizobia that can form nodules with their host plants without the need for nodulation factors. Additionally, they also possess the ability to photosynthesize. This research study has a research hypothesis that during the long and complex evolutionary process, the functional genomes of *Bradyrhizobium*, such as nitrogen fixation genes, photosynthesis genes, and T3SS genes, must have undergone great changes, which makes AIRs form a separate branch that differs significantly from other *Bradyrhizobium*

traits in the phylogenetic tree [9]. The purpose of this research is to figure out the changes that occurred in the genome of AIRs, investigate the diverse origins and evolutionary history of AIRs, and establish a solid theoretical basis for further understanding the phylogeny and genealogy of AIRs; the genomes of AIRs and the reference strains of *Bradyrhizobium* were compared in the present study.

## 2. Materials and Methods

### 2.1. Selection of Test Strains

The complete genome map of strain *B. oligotrophicum* S58<sup>T</sup> was readily accessible in the GenBank database. In this study, we conducted second-generation sequencing on 19 representative strains of AIRs and on *B. denitrificans* LMG8443<sup>T</sup>. The genome sequences were obtained from GenBank, serving as a reference for our comparative genomic analysis with the genome of AIRs. Based on their symbiotic characteristics, *Bradyrhizobium* strains were categorized into three groups: AIRs nodulating with *A. indica* (including CI-I, CI-II, and CI-III types); non-AIRs associating with legumes other than *A. indica*; and non-symbiotic *Bradyrhizobium* lacking the ability to nodulate. The genomes utilized in this study are detailed in Table S1.

### 2.2. Genome Sequencing, Splicing, Optimization

To harvest the biomass, each of the bacterial solutions was centrifuged in a cryogenic centrifuge at 4 °C and 8000 rpm. The collected pellet was frozen and dispatched to Shanghai Meiji Biomedical Technology Co company (Shanghai, China) for comprehensive sequencing. The gene sketches were sequenced on the Illumina (San Diego, CA, USA) second-generation sequencing platform at a depth of 100×. Subsequently, the genome sketches were assembled using SPAdes software (v3.15.5) [33]. Pilon software (v1.23) [34] was employed to refine the genome based on the second-generation sequencing data. Through a comparison of Illumina sequencing data with the genome, Pilon software (v1.23) was employed to generate a BAM file and a genomic FASTA file as input. To assess the genetic relatedness, Average Nucleotide Identity (ANI) values were computed using OrthoANI software (<http://www.ezbiocloud.net/sw/oat>) [35]. This involved pairwise comparisons of genomes, and the results were aggregated to form an ANI matrix. For constructing species trees, OrthoFinder2 software was utilized [36]. The tree file was opened using FigTree software (v1.4.3), and the results were subsequently optimized with iTOL software (v5) [37].

### 2.3. Genome Prediction, Annotation

For predicting genomic functional genes, we employed Prodigal software (v2.6.3) [38]. To annotate the functionality of these genes, we utilized DIAMOND software (v4.6.3) [39]. This annotation process involved referencing the Nr database and the Swiss-Prot database [40,41]. For the analysis of homologous gene families, we turned to OrthoFinder software (v2.0.0).

### 2.4. Analysis of Functional Gene Components

A comprehensive analysis of the functional genes related to the symbiotic process was conducted in AIRs. The genes implicated in symbiosis encompass symbiotic genes, *nif* genes, T3SS genes, T3SS effectors, and photosynthetic genes. Utilizing the BlastGUI software (<https://github.com/byemaxx/BlastGUI>) [35], gene comparisons were performed to construct a library. Subsequently, the results were extracted and organized using a custom Python (v3.10.8) script, allowing us to create a comparative heat map. To conduct covariance analysis of the *nif* gene clusters, genome annotation was carried out for *B. oligotrophicum* S58. Subsequently, the locations of *nif* gene clusters in the annotation file were identified by extracting these clusters from the genomic species of *B. oligotrophicum* S58 for constructing a database. All strains were screened with BlastGUI [35] to identify the existence of *nif* gene clusters. Following the results of the BLAST comparison, appropriate strains harboring the *nif* gene clusters were selected for creating a circos map to visualize and analyze the

differences in *nif* gene clusters among the selected strains, taking *B. oligotrophicum* S58 as reference. Using a similar methodology, covariance analysis of the photosynthetic gene clusters was also conducted. This allowed us to generate a comparative genomic analysis of representative strains of AIRs, with the genome of *B. oligotrophicum* S58<sup>T</sup> serving as the reference. The findings were then presented using Galactic Circos ([usegalaxy.eu](http://usegalaxy.eu), accessed on 26 April 2024) for clarity [42].

### 2.5. Evolutionary Analysis of AIRs

The evolutionary history of AIRs was explored through an analysis involving the species tree and statistical assessments of homologous gene families within the reference strains of AIRs and *Bradyrhizobium*. This analysis was executed using the Count software ([http://www.iro.umontreal.ca/~csuros/gene\\_content/count.html](http://www.iro.umontreal.ca/~csuros/gene_content/count.html)). Subsequently, we utilized Count to analyze the differentiation of AIRs into three specific nodes. Specifically, we identified gene families in which acquisition and loss events occurred at these nodes. Subsequently, these gene families were subjected to KEGG (Kyoto Encyclopedia of Genes and Genomes) analysis to determine if they were enriched in specific metabolic pathways [43].

## 3. Results and Discussion

### 3.1. Genome Profile

The sketch of the genome of AIRs was sequenced, and the genome profile is shown in Table 1. The genome size of AIRs ranged from 6.63 M in the case of *Bradyrhizobium* sp. VII 81001 to 8.84 M in the case of *B. denitrificans* 80005. The GC content of the genomes ranged from 64.55% for *Bradyrhizobium* sp. I 82044 to 65.78% *Bradyrhizobium* sp. IV 81033.

**Table 1.** General data of *Bradyrhizobium* genomes employed in this study.

Strain	Scaffolds	Longest Scaffold	Genome Size	(G + C)%	N90
<i>Aeschynomene indica</i> rhizobia					
<i>B. denitrificans</i> 80005	168	478,427	8.8 M	64.58	47,941
<i>B. oligotrophicum</i> 80025	66	1,331,888	7.9 M	65.22	175,316
<i>B. oligotrophicum</i> LMG8443 <sup>T</sup>	102	491,180	8.3 M	64.75	55,376
<i>B. oligotrophicum</i> S58 <sup>T</sup>	1	8,264,165	8.3 M	65.13	8,264,165
<i>Bradyrhizobium</i> sp. I 82044	45	880,514	6.9 M	64.55	113,255
<i>Bradyrhizobium</i> sp. I 82054	58	887,869	7.0 M	64.62	72,231
<i>Bradyrhizobium</i> sp. II 80013	65	819,284	7.2 M	64.83	117,592
<i>Bradyrhizobium</i> sp. III 80001	141	712,781	7.7 M	65.67	35,344
<i>Bradyrhizobium</i> sp. IV 81033	59	711,146	7.5 M	65.48	113,462
<i>Bradyrhizobium</i> sp. V 80016	75	979,362	7.8 M	65.00	136,370
<i>Bradyrhizobium</i> sp. V 80022	54	2,692,961	7.8 M	65.02	252,498
<i>Bradyrhizobium</i> sp. V 80029	80	1,354,028	7.9 M	65.00	247,781
<i>Bradyrhizobium</i> sp. VI 80004	61	671,467	7.9 M	64.77	106,416
<i>Bradyrhizobium</i> sp. VII 81001	112	619,092	6.6 M	65.48	45,649
<i>Bradyrhizobium</i> sp. VII 81035	100	769,653	7.1 M	65.62	83,941
<i>Bradyrhizobium</i> sp. VII 82079	69	676,485	7.4 M	65.42	80,746
<i>Bradyrhizobium</i> sp. VII 82084	52	1,331,153	7.5 M	65.48	125,140
<i>Bradyrhizobium</i> sp. VIII 81003	46	1,209,915	7.4 M	65.78	130,606
<i>Bradyrhizobium</i> sp. VIII 81013	58	768,856	7.5 M	65.51	155,814
<i>Bradyrhizobium</i> sp. VIII 83002	59	1,045,725	7.5 M	65.42	150,740
<i>Bradyrhizobium</i> sp. VIII 83012	58	1,487,792	7.5 M	65.54	115,572
<i>Bradyrhizobium</i> sp. ORS 278	1	7,456,587	7.5 M	65.51	7,456,587
<i>Bradyrhizobium</i> sp. ORS 285	301	212,771	7.6 M	65.23	13,681
<i>Bradyrhizobium</i> sp. DOA9	2	7,114,464	7.9 M	64.49	7,114,464
Non- <i>A. indica</i> symbiotic rhizobia					
<i>B. arachidis</i> LMG26795 <sup>T</sup>	98	839,589	9.8 M	63.63	70,254
<i>B. cytisi</i> CTAW11 <sup>T</sup>	186	436,932	8.9 M	63.17	35,919
<i>B. daqingense</i> CGMCC1.10947 <sup>T</sup>	107	742,797	7.9 M	63.73	38,665
<i>B. diazoefficiens</i> USDA110 <sup>T</sup>	1	9,105,828	9.1 M	64.06	9,105,828
<i>B. elkanii</i> USDA76 <sup>T</sup>	2	9,116,505	9.5 M	63.72	9,116,505

Table 1. Cont.

Strain	Scaffolds	Longest Scaffold	Genome Size	(G + C)%	N90
<i>B. embrapense</i> SEMIA6208 <sup>T</sup>	36	1,556,835	8.3 M	63.98	139,684
<i>B. guangdongense</i> CCBAU51649 <sup>T</sup>	2	7,456,045	8.4 M	63.26	981,946
<i>B. guangxiense</i> CCBAU53363 <sup>T</sup>	2	7,220,948	8.2 M	63.91	979,173
<i>B. icense</i> LMTR13 <sup>T</sup>	1	8,322,773	8.3 M	62.03	8,322,773
<i>B. japonicum</i> USDA6 <sup>T</sup>	1	9,207,384	9.2 M	63.67	9,207,384
<i>B. jicamae</i> PAC68 <sup>T</sup>	235	238,143	8.7 M	62.40	22,567
<i>B. lablabi</i> CCBAU23086 <sup>T</sup>	135	408,238	8. M	62.63	33,805
<i>B. liaoningense</i> CCBAU05525 <sup>T</sup>	1040	62,700	8.1 M	63.80	4068
<i>B. manausense</i> BR3351 <sup>T</sup>	127	850,526	9.1 M	62.87	47,046
<i>B. mercantei</i> SEMIA6399 <sup>T</sup>	72	1,570,373	8.8 M	63.99	259,995
<i>B. neotropiale</i> BR10247 <sup>T</sup>	125	440,229	8.7 M	63.60	42,996
<i>B. ottawaense</i> OO99 <sup>T</sup>	1	8,606,328	8.6 M	63.83	8,606,328
<i>B. stylosanthis</i> BR 446 <sup>T</sup>	22	2,454,055	8.8 M	64.56	237,570
<i>B. viridifuturi</i> SEMIA690 <sup>T</sup>	152	399,926	8.8 M	64.03	50,014
<i>B. yuanningense</i> CCBAU10071 <sup>T</sup>	108	1,099,763	8.2 M	63.77	37,101
Non-symbiotic <i>Bradyrhizobium</i>					
<i>B. betae</i> PL7HG1 <sup>T</sup>	2	7,150,095	7.41 M	64.36	7,150,095
<i>Bradyrhizobium</i> sp. AT1	8	7,515,445	7.5 M	64.56	7,515,445
<i>Bradyrhizobium</i> sp. BF49	1	7,547,693	7.5 M	63.77	7,547,693
<i>Bradyrhizobium</i> sp. G22	20	9,022,917	9.1 M	63.73	9,022,917
<i>Bradyrhizobium</i> sp. LTSP849	57	599,414	8.5 M	63.24	131,906
<i>Bradyrhizobium</i> sp. LTSP857	50	993,329	8.4 M	63.29	106,609
<i>Bradyrhizobium</i> sp. LTSP885	43	1,049,129	7.9 M	63.39	116,147
<i>Bradyrhizobium</i> sp. LTSPM299	100	682,398	9.1 M	62.82	59,442
<i>Bradyrhizobium</i> sp. OK095	51	1,094,326	7.8 M	63.89	157,651
<i>Bradyrhizobium</i> sp. S23321	1	7,231,841	7.2 M	64.30	7,231,841
<i>Bradyrhizobium</i> sp. URHA0002	144	405,618	7.0 M	62.20	26,273
<i>Bradyrhizobium</i> sp. YR681	351	167,815	7.8M	64.72	11,443

<sup>T</sup> indicates that the strain is a Type strain.

The large variation in genome size of AIRs, which is consistent with previous studies [44–52], suggests a long evolutionary history, leading to divergence in genome size. Variations in mean genome size were observed among different classes of *Bradyrhizobium*. The average genome size is 7.6 M for AIRs, 8.7 M for non-AIRs, and the average genome size is 8.0 M for non-symbiotic *Bradyrhizobium*, which might be related to distinct selection pressures from their hosts and environments on these three classes of rhizobia [53].

### 3.2. Analysis of the Origin of AIRs

Orthologous gene family (orthogroup) analysis revealed that a total of 421,466 genes were identified in the genomes of 56 tested *Bradyrhizobium* strains, which were organized into 17,858 gene families. Out of all the genes, 408,370 (96.9%) were assigned to these gene families, while 13,096 genes (3.1%) were found in only one strain. Additionally, there were 36 specific gene families encompassing 95 genes (less than 0.1%). Furthermore, 2074 orthogroups presented in all the 56 *Bradyrhizobium* strains, and 1098 of these were single-copy gene families.

A species tree was constructed based on 56 homologous gene families of AIRs (Figure 1). In Figure 1, the tested strains in *Bradyrhizobium* were clearly divided into three branches, with AIRs located in two of them. The 20 strains in Cluster I were all able to nodulate with Indian AIRs. In this cluster, *Bradyrhizobium* sp. ORS285 is a CI-II type photosynthetic strain, which could form root and stem nodules with *Aeschynomene* species via NF-dependent and NF-independent mechanisms [54]. No AIR strain was included in Cluster II, which consisted mainly of non-symbiotic *Bradyrhizobium* strains and *Bradyrhizobium* strains that nodulate with other legumes. Four strains of AIRs were grouped in Cluster III, in which *Bradyrhizobium* sp. I 82044, 82054, and *Bradyrhizobium* sp. II

80013 were isolated for this study, while *Bradyrhizobium* sp. DOA9 was a CI-I type strain nodulating *A. indica* but originally isolated from America and could fix nitrogen in free living conditions [54]. In Cluster III, *Bradyrhizobium* sp. I 82044, 82054, and *Bradyrhizobium* sp. II 80013 are clustered in a small branch together with *B. liaoningense* and *B. yuanmingense*. The hosts of *B. liaoningense* include peanut, a legume species infected by bradyrhizobia via root cracks. Furthermore, *B. liaoningense* also shared the same geographic distribution with the three isolates of AIRs in this study. The close kinship between the hosts, the consistent infestation pattern in both rhizobia nodulation processes, and the similar geographic locations suggest that *Bradyrhizobium* sp. I and *B. liaoningense* share a common ancestor, with the two *Bradyrhizobium* strains differentiating later throughout their subsequent long-term and complex evolutionary history, as reported in other studies [55–57]. The original host of *Bradyrhizobium* sp. DOA9 and *B. yuanmingense* were close relatives in Figure 1, and their symbiotic nodulation relied on the exchange of nodulation factors. In cluster III, *Bradyrhizobium* sp. II 80013 presented a close relationship with non-symbiotic *Bradyrhizobium* strain *Bradyrhizobium* sp. S23321 isolated from the rhizosphere of rice. Moreover, *B. betae* PL7HG1 (isolated from the beetroot sphere) [58], *Bradyrhizobium* sp. YR681, and *Bradyrhizobium* sp. OK095 (isolated from the poplar rhizosphere) [59] also have very similar phylogenetic positions to 80013 (Figure 1), indicating a possible origin of *Bradyrhizobium* sp. II 80013 from non-symbiotic *Bradyrhizobium*.

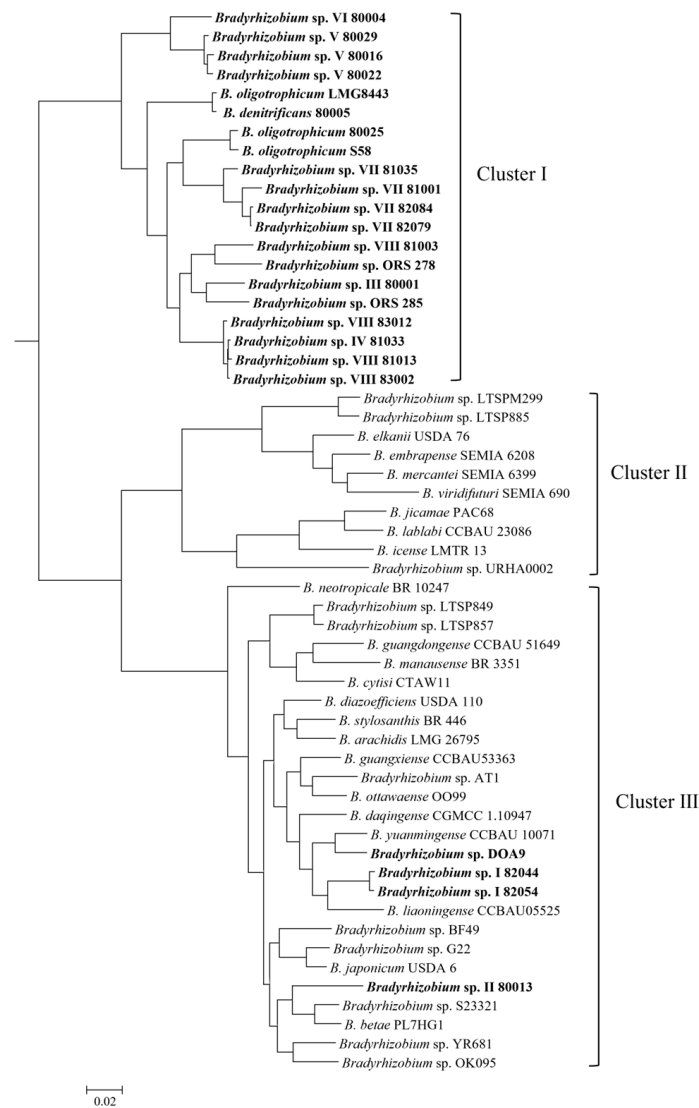


Figure 1. The phylogenetic tree based on homologous gene families of *Bradyrhizobium* strains.

Based on the phylogenetic relationships in Figure 1, it is speculated that AIRs can be categorized into three origin modes. The first mode involves AIRs originating from the early differentiation of *Bradyrhizobium* species (cluster I), which has a long evolutionary history and has accumulated great genetic variations, resulting in a high level of diversity. This is evidenced by the significant differences in genome size and GC content, as well as the formation of cluster I as a separate and highly differentiated branch in the species tree (Figure 1) of housekeeping genes. The second group covers the strains *Bradyrhizobium* sp. DOA9 and *Bradyrhizobium* sp. I 82044 and 82054, which originated relatively later from species of non-AIRs and might share an ancestor with the peanut rhizobia since the nodulation mode of all rhizobia with peanut is fissure infection [60], which is conducive to the mutual transformation of their symbiotic bacteria. The third group, represented by *Bradyrhizobium* sp. 80013, might have originated from non-symbiotic *Bradyrhizobium* in the soil and cannot synthesize nodulation factors, but some strains have photosynthetic ability. The above traits overlap with AIRs and can be easily selected and differentiated into AIRs by nodulating *A. indica*. The low diversity of the second and third groups suggests that they have evolved recently.

### 3.3. Comparative Genome Analysis of AIRs

The different origins of AIRs have necessarily undergone distinct evolutionary histories, potentially resulting in significant differences in their genome components. To investigate these differences, a comparative genomic analysis was conducted on three different origins of AIRs.

*Bradyrhizobium* sp. VIII 83002 belongs to the branch of Cluster I, which exhibits early formation and high diversity. AIRs within this branch appear to share similarities due to the selection pressure of the host and, as a result, correspond closely to the genomic components of 83002, characterized by the presence of a large number of contiguous fragments. *Bradyrhizobium* sp. III 80001 has the smallest genome, but it has more gaps than 83002. Both 80001 and *Bradyrhizobium* sp. ORS285 are clustered in the same branch on the species tree, and the original host of ORS285 was the CI-II type of *A. indica*, which contains the Nod gene. Therefore, 80001 likely originated from the CI-II type of *A. indica* and underwent a large number of gene loss events to adapt to an NF-independent nodulation mode. *Bradyrhizobium* sp. VIII 83002 has differentiated significantly from non-*A. indica* rhizobia (*B. yuanmingense* CCBAU10071), non-symbiotic *Bradyrhizobium* (*B. betae* PL7HG1, *Bradyrhizobium* sp. S23321), and Cluster III-branched AIRs (*Bradyrhizobium* sp. I 82044, *Bradyrhizobium* sp. II 80013), with substantial differences in genomic components and poor genomic covariance. Genome 83002 has several regions with low GC content (indicated by black arrows in the figure), and gaps exist in other strains, suggesting that HGT has occurred in these regions (Figure 2A). *Bradyrhizobium* sp. II 80013 is a strain of AIRs in the Cluster III branch, forming a small sub-branch alongside non-symbiotic *Bradyrhizobium* in the species tree. The 80013 genome is characterized by the presence of numerous significant endemic segments (indicated by black arrows in the figure), and the GC content of these regions suggests that horizontal gene transfer has occurred, along with significant changes in the genome structure during the transformation of 80013 into AIRs (Figure 2B). *Bradyrhizobium* sp. I 82044 is also identified as an AIR within Cluster III. According to the *Bradyrhizobium* species tree, it is assumed that this strain originated from the transformation of a non-symbiotic *Bradyrhizobium*. The genome of *Bradyrhizobium* sp. I 82044 also contains regions with a low GC content (indicated by black arrows in the figure). However, these regions are not unique to 82044, suggesting that they may have originated from AIRs. The average genome size of non-AIRs is 8.7 M, while that of 82044 is only 6.9 M. This size difference suggests that the transformation of 82044 into *A. indica* was accompanied by the loss of a significant number of genomic fragments. These fragments may include genes associated with the host symbiosis of 82044's ancestors, aligning with the possible origin of 82044 from non-AIRs (Figure 2C).

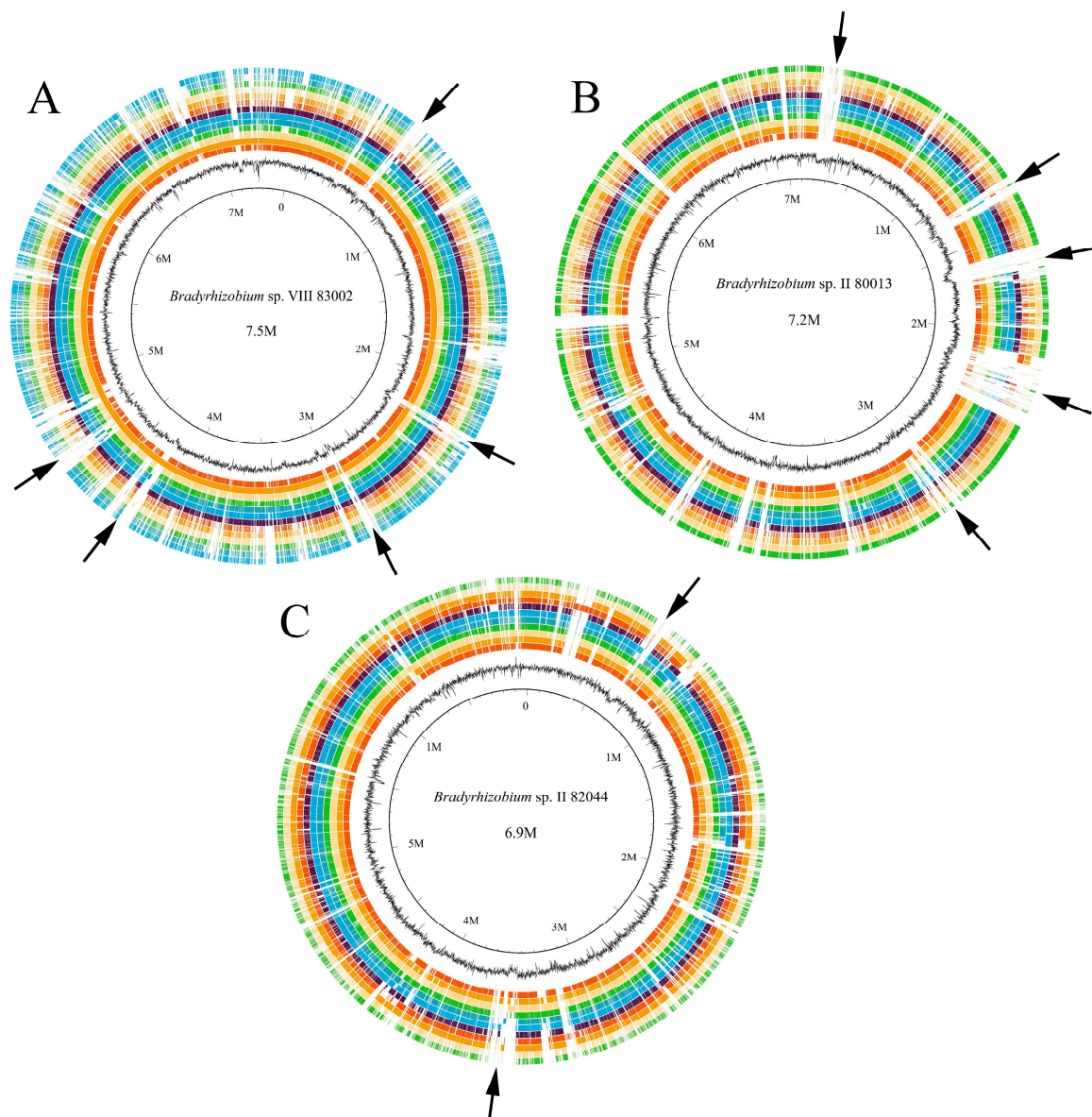


**Figure 2.** Comparative genomic analysis of *Bradyrhizobium* strains associated with *A. indica* from diverse geographical origins. (A). The circles from inside to outside correspond to strains *Bradyrhizobium* sp. VIII 83002, GC%, sp. III 80001, sp. IV 81033, sp. V 80016, sp. VI 80004, sp. VII 82079, *B. denitrificans* 80005, *B. oligotrophicum* 80025, sp. DOA9, sp. I 82044, *B. yuanmingense* CCBAU10071, sp. II 80013, *B. betae* PL7HG1<sup>T</sup>, sp. S23321. (B). The circles from inside to outside are *Bradyrhizobium* sp. 80013, GC%, *B. betae* PL7HG1<sup>T</sup>, sp. S23321, sp. AT1, sp. G22, sp. LTSP849, sp. YR681, sp. I 82044, sp. VII 82079, sp. VIII 83002, *B. cytisi* CTAW11<sup>T</sup>, *B. japonicum* USDA6<sup>T</sup>. (C). The circles from inside to outside are *Bradyrhizobium* sp. II 82044, GC%, *B. liaoningense* CCBAU05525<sup>T</sup>, *B. yuanmingense* CCBAU10071<sup>T</sup>, *B. daqingense* CGMCC1.10947<sup>T</sup>, *B. ottawaense* OO99<sup>T</sup>, *B. stylosanthis* BR446<sup>T</sup>, *B. guangxiense* CCBAU53363<sup>T</sup>, sp. II 80013, *B. betae* PL7HG1<sup>T</sup>, sp. S23321, sp. VII 82079, sp. VIII 83002. Black arrow means the GC content of this region is very low.

HGT occurs in several regions of the genome of AIRs. There are three main forms of HGT [61]. First is transformation, in which AIRs take up naked DNA fragments directly from the environment, integrate them into their own genome, and perform their functions. However, the low concentration of DNA fragments in the environment makes the transformation process difficult to observe, and it can only be deduced backwards from phylogenetic trees or genomic information. Second, conjugative transfer occurs [62–64],

which is the process of DNA transfer between the donor and the recipient bacterium through contact. The DNA fragments are recombined at the *att* site (usually one of the loci is adjacent to *phe*-tRNA) by the action of integrase and transferred via T4SS [63]. This process requires a high structural basis for the genome, and the analysis of the genome of *A. indica* in this study did not reveal any relevant structures at either end of the low GC fragment. Furthermore, the absence of the T4SS-encoding gene in AIRs does not support DNA translocation. Third, phage-mediated horizontal gene transfer [65–67] occurs, in which phages take the genomic DNA of the former host and integrate it into the next host when they infest between different bacteria. The presence of prophage integrase in the genome of AIRs suggests that phages play a role in the horizontal gene transfer of AIRs.

### 3.4. Analysis of Symbiotic Nitrogen Fixation Gene Components

Nod genes encode enzymes for nodulation factor (NF) synthesis, and rhizobia with nodulation capacity generally have the *nodABC* genes for synthesis of the main structure of NF, as well as a number of genes for modifying the NF. Most of the AIR strains in clusters I and II, except *Bradyrhizobium* sp. DOA9 and *Bradyrhizobium* sp. ORS 285, only harbored *nodN* and *nodQ*, while several of them also harbored *nodM* and *nodP1/nodP2* but were absent for the regulation and construction *nod* genes (Figure 3). A similar situation was observed in the 12 non-symbiotic *Bradyrhizobium* strains. Among the AIR strains, *Bradyrhizobium* sp. DOA9 and *Bradyrhizobium* sp. ORS 285, which nodulate with CI-I and CI-II types of *Aeschynomene* species, respectively, contain all the essential conserved genes for nodulation factor synthesis in their genomes, demonstrating they are symbionts with an NF-dependent strategy, which is similar to the *Bradyrhizobium* strains nodulating with other legume species (Figure 3). It was interesting that all the 56 tested *Bradyrhizobium* strains in this study contained *nodN* and *nodQ* genes, demonstrating that they may also play some essential role in a pathway(s) without relation to symbiosis. For example, *nodM* and *nodN* genes present common functions as glucosamine synthase, playing a crucial role in the biosynthesis of hexosamine [68], while *nodO* gene encodes a hemolysin homolog [69].

The *nif* (*Nif*) genes were more widely distributed than Nod genes in *A. indica*-nodulating bradyrhizobia. As shown in Figure 4, *nifHDKNEX* genes were harbored in the genomes of all the tested symbiotic *Bradyrhizobium* strains except *Bradyrhizobium* sp. VII 81001, suggesting that all of these gene strains possessed the potential of *nif*. Our previous study has indicated that mutations contribute more to evolution than recombination [1]. Strain 81001 has a genome size of only 6.1 M, which is the smallest among *A. indica*-nodulating strains, suggesting that this strain has undergone a large number of gene loss events during its evolutionary history, and *nif* genes were lost at some point (Figure 4). Nitrogen fixation is a very energy-intensive biological process [70,71], and the ability of rhizobia to fix nitrogen does not contribute significantly to the environmental adaptability and competitiveness of *Bradyrhizobium* when they are saprophytic in soil; as a result, most non-symbiotic strains do not have *Nif* genes in their genomes. *Bradyrhizobium* sp. S23321 and *Bradyrhizobium* sp. AT1 were found to have a more complete cluster of nitrogen fixation genes [72], suggesting that the ancestors of these two strains may have had the ability to have symbiosis with legumes.

In most cases, *Nif* genes presented a co-evolutionary tendency with *nod* genes, and host specificity was observed since *Nif* genes from the same host can often transcend phylogenetic boundaries and cluster in the same branch. Among the *nif* gene clusters of AIRs, *nifHDKNEX* is a conserved *nif* gene operon and is consistently arranged in the same order in different bacteria. In this study, a phylogenetic tree was constructed for *NifHDKNEX* gene clusters to analyze their evolution (Figure 5). *B. oligotrophicum* S58<sup>T</sup> has been sequenced, and the *nif* gene Cluster I is located in the region spanning 2584552' to 2632812', with a total length of 48,270 bp. This strain was used as a reference for a comparative analysis of the *nif* genomic score of *Bradyrhizobium*. The phylogenetic tree depicts the *nifHDKNEX* gene clustering into three distinct branches, consistent with that defined in Figure 1. AIRs within Branch I covered all strains in Cluster I of Figure 1

and separated from the other *Bradyrhizobium* species, suggesting a common origin for the *Nif* genes in this branch, with an evolutionary history distinguished from the other *Bradyrhizobium* species. It further supports the idea that *Bradyrhizobium* within Branch I has a unique origin. Additionally, *nif* capacity is a crucial component of the mutually beneficial symbiotic system. The *nif* gene experiences more significant host selection pressure than even the nodulation gene. Within the Branch I, the *nif*DKNEX branch appears to be more diverse and abundant, indicating a longer evolutionary history for this particular branch. *Bradyrhizobium* sp. I 82044, 82054, *Bradyrhizobium* sp. II 80013, and *Bradyrhizobium* sp. DOA9 harbor the *nif*DKNEX genes distinct from that of AIRs in the branch of Cluster I but more similar with that of *B. guangxiense*, suggesting that their *nif*DKNEX genes have origins different from those in Cluster I. The *nif*DKNEX genes on the chromosome of *B. guangxiense* presented closer phylogenetic relationships to those of *Bradyrhizobium* sp. I 82044, 82054, and *Bradyrhizobium* sp. DOA9, suggesting that they might have the same origin. A previous study evidenced that *B. guangxiense* can cross-nodulate with Indian *A. indica*, further demonstrating that non-AIRs could be transformed into AIRs. The phylogenetic tree based on the *Nif*DKNEX genes shows that *B. liangningense* is distantly related to *Bradyrhizobium* sp. I 82044, 82054, and *Bradyrhizobium* sp. DOA9. Instead, they were clustered together with other *Bradyrhizobium* strains that share the same host, suggesting the existence of HGT of *nif* genes in *B. liangningense*. In this study, the *nif* gene cluster was only found in *Bradyrhizobium* sp. S23321 and *Bradyrhizobium* sp. AT1, both of which clustered in the same branch as *Bradyrhizobium* sp. II 80013 in the phylogenetic tree. This finding further demonstrates that *Bradyrhizobium* sp. II 80013 is more closely related to non-symbiotic *Bradyrhizobium*. The position of AIRs in the *nif*DKNEX phylogenetic tree closely corresponds to the species tree (Figure 5). AIR strains of the same genetic species cluster in the same branch, indicating that the *nif* genes of AIRs are primarily transmitted vertically, which is highly in accordance with previous research [6].

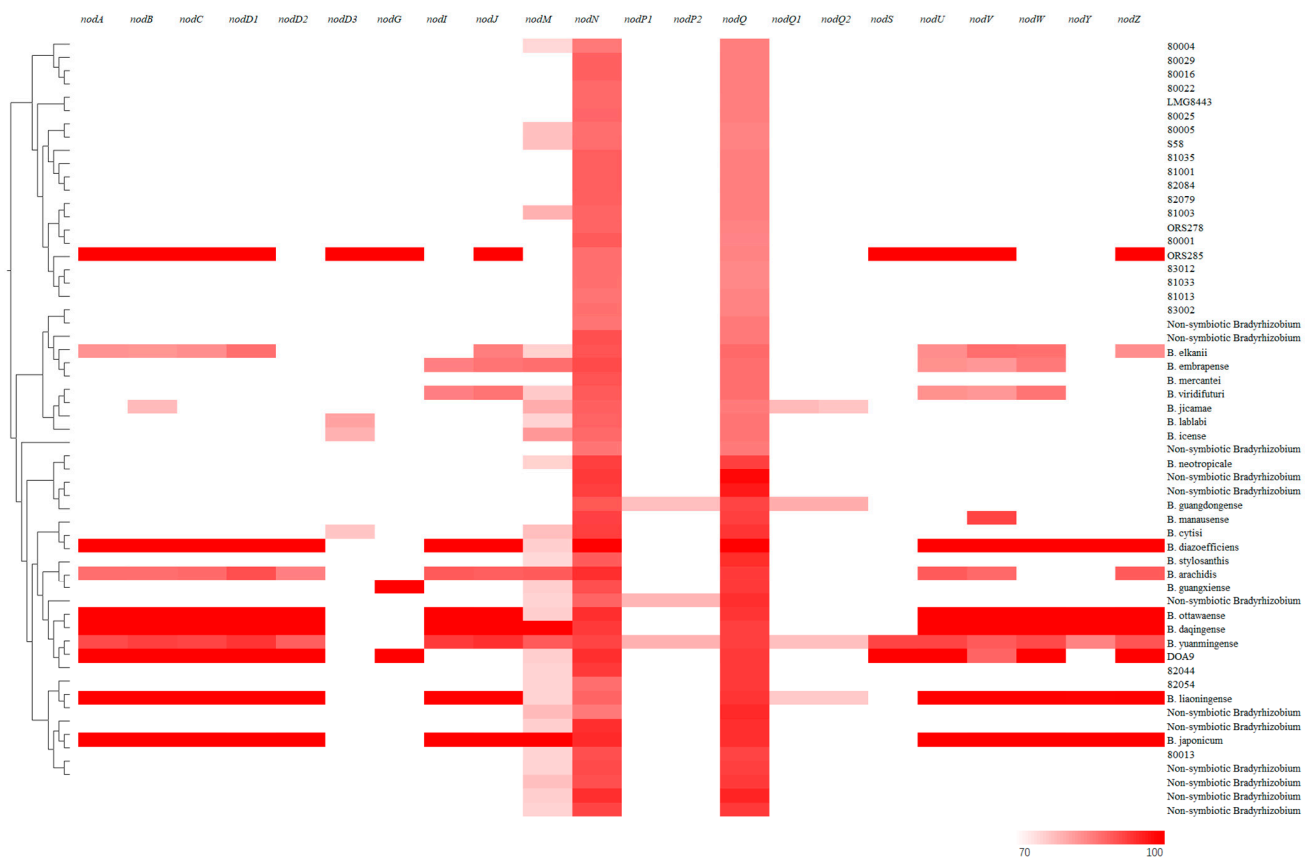
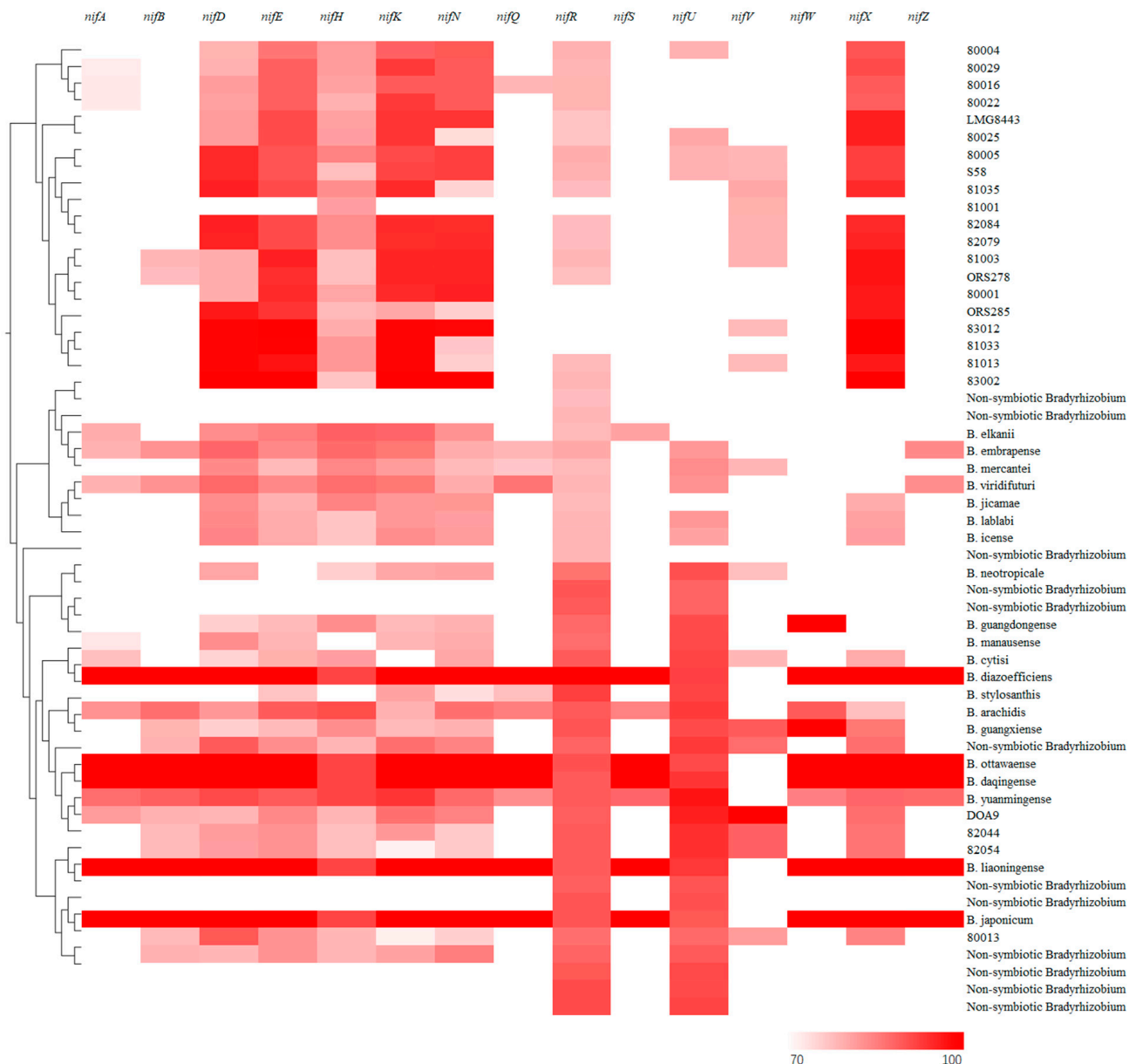
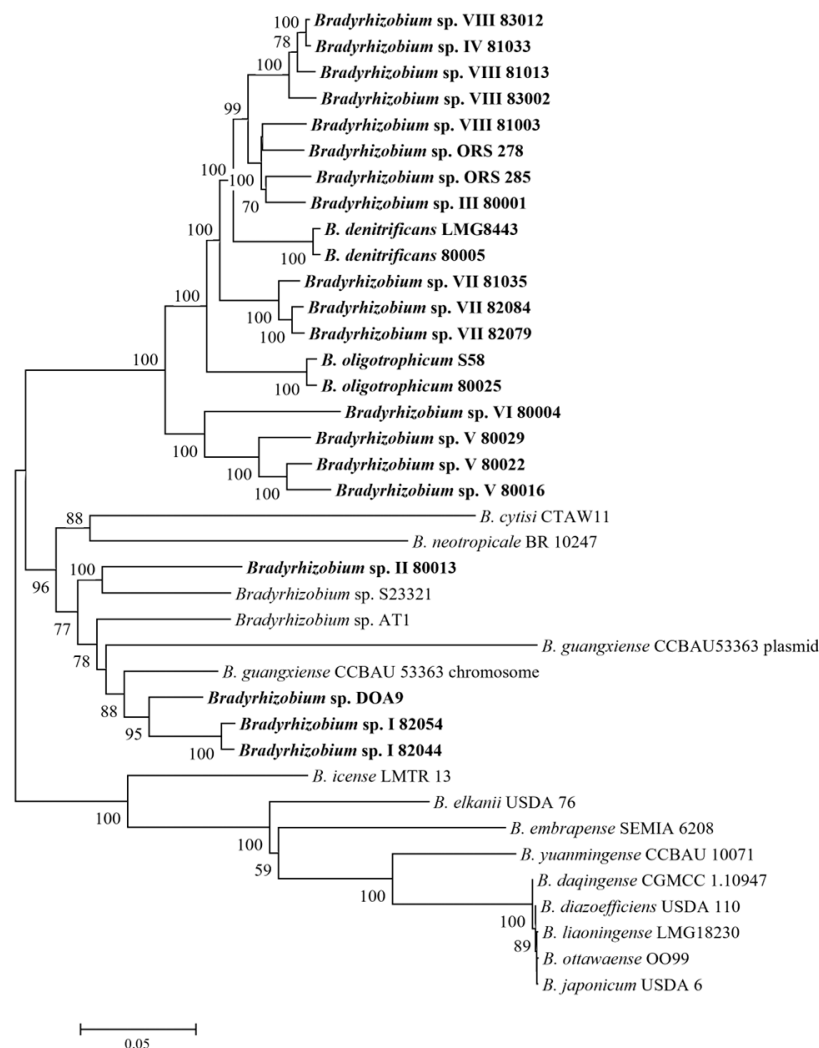


Figure 3. Analysis of nodulation gene components in *Bradyrhizobium*.



**Figure 4.** Analysis of nitrogen fixation gene components of *Bradyrhizobium*.

The *B. oligotrophicum* S58<sup>T</sup> *nif* gene cluster is 48,270 bp in length, with an average GC content of 64.11%, ranging from 47% to 80% GC per 100 bp [12]. The gene cluster contains 64 genes encoding *nif* molybdenum iron proteins, *nif*-related transporter proteins, and regulatory proteins. The S58 *nif* gene Cluster I is almost identical to the component of AIRs of Cluster I. The strains in the branch of Cluster III differ from S58 in their *nif* gene cluster components. The *nif* gene cluster components of *Bradyrhizobium* sp. I 80013 (transformation origin of non-AIRs) and *Bradyrhizobium* sp. II 82044 and 82054 (origin of non-symbiotic *Bradyrhizobium*) are consistent, indicating that both types of AIRs have the same origin of *nif* genes. Compared to strain S58, only 17.5% of the *nif* gene clusters in *B. japonicum* USDA 6 exhibit consistency, implying greater divergence in *nif* gene clusters among *Bradyrhizobium* in association with different hosts. *B. betae* PL7HG1, isolated from sugar beet roots [58], contains a minimal number of nitrogen-fixing genes and lacks nitrogen-fixing capacity, with just 4.7% of its genetic sequence aligning with the *nif* gene cluster of strain S58. The high collinearity observed in the *nif* gene clusters among closely related strains suggests that these *nif* genes in AIRs primarily undergo vertical transmission (Figure 6).



**Figure 5.** Phylogenetic tree of *Bradyrhizobium nifDKNEX* gene cluster.

It is evident that nitrogen fixation genes (*nif* genes) are highly conserved in AIRs and show high covariance among different strains, which suggests that these genes are mainly transmitted through vertical rather than horizontal gene transfer (HGT). However, HGT still plays a role in AIRs. This is important for understanding the evolution of AIRs, as it indicates the strong pressure of host selection on these genes during symbiosis. In addition, our study showed that the *nif* gene clusters of different strains exhibited some differences in composition and arrangement, which may be related to the ecological environment and biological characteristics of different host plants. Although some strains lost some of their *nif* genes during evolution, the majority of these gene clusters retained and maintained their functions.

### 3.5. Analysis of Photosynthetic Gene Components

Bacterial chlorophylls, carotenoids, and photoreaction centers are the structural basis for photosynthesis in *Bradyrhizobium* [73]. In this study, we analyzed the components of thirteen bacterial chlorophyll-encoding genes, six carotenoid-encoding genes, and nine photoreaction center-encoding genes in *Bradyrhizobium* (Figure 6), which were extracted from the genomes. Among the 16 strains of AIRs in Cluster I, only *Bradyrhizobium* sp. VI 80004 lacked a complete set of photosynthetic genes in its genome. In Cluster III, the genomes of *Bradyrhizobium* sp. I 82044 and 82054 contained partial bacterial chlorophyll (*bch*)- and carotenoid (*crt*)-coding genes but lacked photoreaction center (*puf*)-coding genes. Conversely, the genome of *Bradyrhizobium* sp. II 80013 included the complete photosyn-

thetic gene set, consistent with the PCR amplification results of the *pufLM* gene. The photosynthetic genome component of non-AIRs exhibited high similarity to strains 82044 and 82054, indicating a close phylogenetic relationship between these groups of *Bradyrhizobium*. This similarity further supports the notion that non-AIRs may represent one of the origins of AIRs. Notably, as demonstrated in a previous study [3], similar results were obtained for the two strains (*B. betae* PL7HG1 and *Bradyrhizobium* sp. S23321) that are most closely related to 80013 in the species tree and contain photosynthetic genes in their genomes [58,72]. This suggests that although the photosynthetic genes of 80013 originated from non-symbiotic *Bradyrhizobium*, they have undergone more substantial modifications in subsequent evolutionary history (Figure 7).

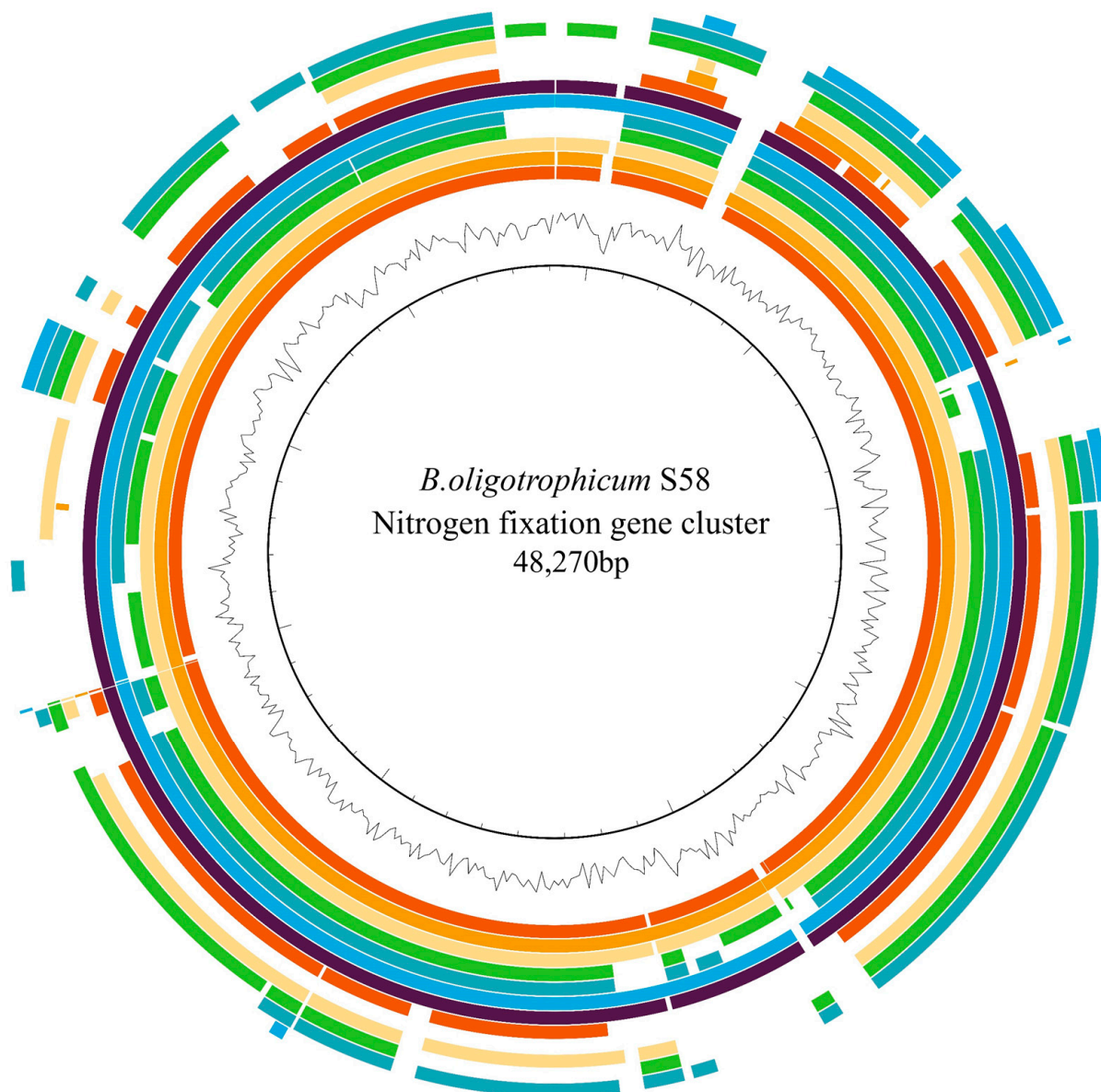


**Figure 6.** Collinearity analysis of nitrogen fixation gene cluster in *Bradyrhizobium*. The circles from inside to outside in circus figure mean: *B. oligotrophicum* S58<sup>T</sup> *nif* gene cluster, S58<sup>T</sup> GC%, *B. oligotrophicum* 80025, *Bradyrhizobium* sp. III 80001, *Bradyrhizobium* sp. IV 81033, *Bradyrhizobium* sp. V 80016, *Bradyrhizobium* sp. VI 80004, *Bradyrhizobium* sp. VII 82079, *Bradyrhizobium* sp. VIII 83002, *Bradyrhizobium* sp. II 80013, *B. betae* PL7HG1, *Bradyrhizobium* sp. S23321, *Bradyrhizobium* sp. I 82044, *B. guangxiense* CCBAU53363, *B. japonicum* USDA 6.

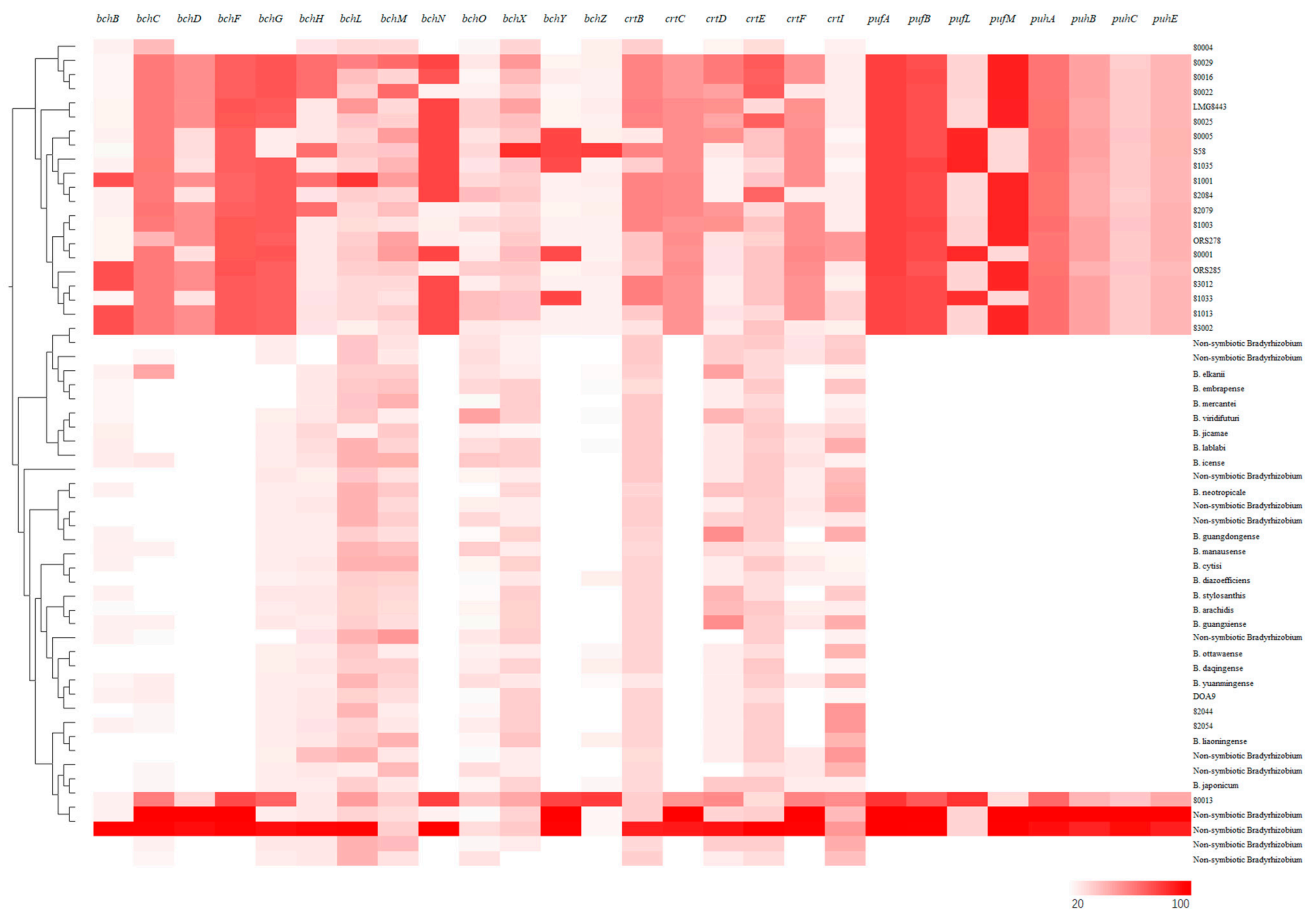


**Figure 7.** Analysis of photosynthetic gene components of *Bradyrhizobium*.

In the genome of AIRs, the composition and arrangement of genomes within the photosynthetic gene cluster vary significantly among strains. To depict the phylogenetic relationships of photosynthetic genes in different strains, chlorophyll-coding genes (*bchF*, *bchG*, *bchN*), carotenoid-coding genes (*crt I*, *crtB*, *crtC*), and photoreaction center-coding genes (*pufA*, *pufB*, *pufL*) were extracted from the genomes of AIRs and reference strains. The sequences of these genes were then concatenated to construct a phylogenetic tree (Figure 8). In Figure 8, *Rhodopseudomonas*, the oldest photosynthetic bacterium on the Earth, is positioned on the outermost branch, suggesting that the photosynthetic capacity of AIRs may have a common origin with *Rhodopseudomonas*. *B. betae* PL7HG1 and *Bradyrhizobium* sp. S23321 are located between *Rhodopseudomonas* and AIRs but closer to *Rhodopseudomonas*, suggesting that non-symbiotic *Bradyrhizobium* strains might be the first within the *Bradyrhizobium* genus to acquire photosynthetic capabilities. Previous studies have demonstrated that the photosynthetic genes of *Bradyrhizobium* were obtained through multiple HGTs [6,9]. Therefore, the initial photosynthetic capacity of AIRs likely originated from the common ancestor with *Rhodopseudomonas* and was subsequently acquired by non-symbiotic *Bradyrhizobium* strains. In Figure 8, strain 80013 is positioned at the outermost part of AIRs and exhibits significant differences from non-symbiotic *Bradyrhizobium* strains, suggesting that strain 80013 acquired photosynthetic genes earlier and accumulated a substantial amount of genetic variation throughout its evolutionary history. With the exception of *Bradyrhizobium* sp. VI 80004, all genomes of AIRs within the Cluster branch exhibit the presence of photosynthetic genes. These genes also display a high level of diversity, indicating their existence during the formation of the common ancestral species of AIRs within this group and their subsequent preservation throughout evolutionary history. It is possible that *Bradyrhizobium* sp. VI 80004 experienced deletions of photosynthetic genes during its own evolutionary trajectory. Interestingly, the phylogenetic tree of photosynthetic genes

in *Bradyrhizobium* sp. VI 80004 closely aligns with the species tree, suggesting that photosynthetic genes are primarily transmitted vertically within AIRs, and no HGT events have been detected (Figure 8).

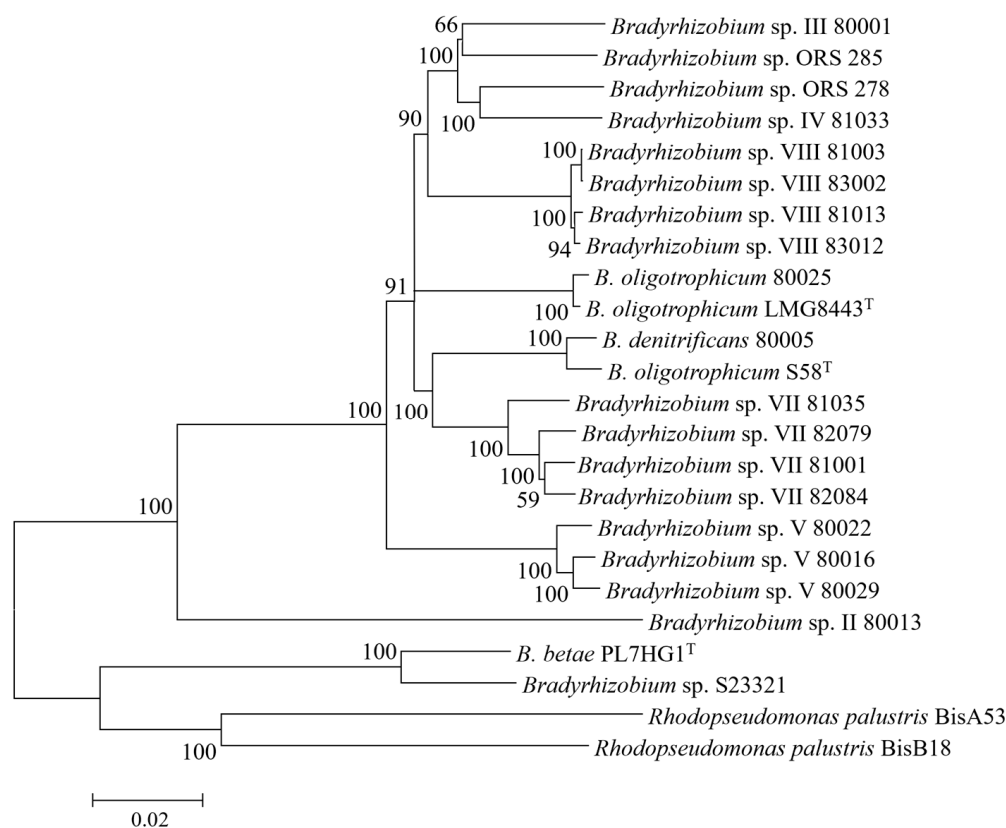


**Figure 8.** Phylogenetic tree of photosynthetic gene concatenated sequences. “<sup>T</sup>” indicates that the strain is a Type strain.

The photosynthetic gene cluster of *B. oligotrophicum* S58<sup>T</sup> is mainly concentrated in a 59,571 bp fragment with an average GC content of 66.77% and GC content between 45% and 80% per 100 bp [12]. The gene cluster contains 53 genes, most of which encode for the synthesis of bacterial chlorophylls, carotenoids, and photoreaction centers. There are also some genes of unknown function in the gene cluster, and whether these genes are related to photosynthesis still needs further study. The results of comparative analysis of symbiotic and non-symbiotic photosynthetic rhizobial strains, as well as the phototrophic gene cluster components of the genus *Bradyrhizobium* and *Rhodopseudomonas*, indicate the phototrophic gene cluster of strain S58 is identical to that of its counterpart strain 80025, which shows a higher degree of collinearity with the components of Cluster I of symbiotic *Bradyrhizobium*, suggesting a shared origin of phototrophic genes in these strains. However, among the genomes studied, only *Bradyrhizobium* sp. II 80013 contains photosynthetic gene clusters in Cluster II. These components differ more significantly from that of S58, displaying more gaps between them. The proportion of congruent components between the two clusters is approximately 76.29%. The *nif* gene cluster in the non-symbiotic strains *B. betae* PL7HG1 and *Bradyrhizobium* sp. S23321, as well as *Rhodopseudomonas palustris* BisA53 and BisB18, exhibit more and larger gaps with that of S58. These gaps correspond to consistency components of 48.99%, 41.53%, 47.76%, and 48.99%, respectively. The higher collinearity observed in the photosynthetic gene clusters of strains with closer phylogenetic relationships suggests that the transmission of photosynthetic genes in AIRs is predominantly vertical. Additionally, the presence of a significant number of gaps in the photosynthetic gene cluster of *Bradyrhizobium* sp. VI 80004 indicates substantial gene losses in this particular strain (Figure 9).

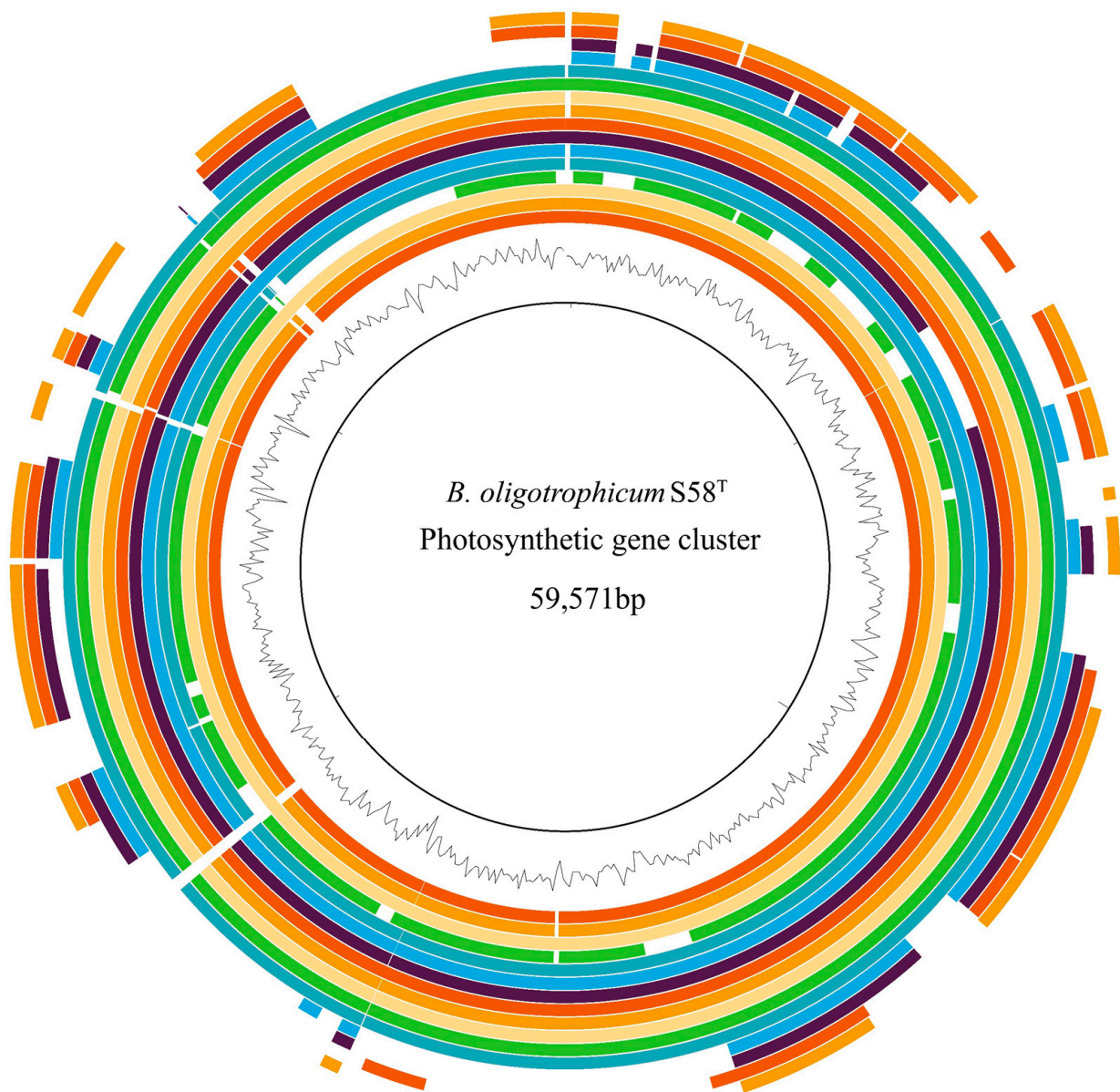


**Figure 9.** Collinearity analysis of photosynthetic gene cluster in *Bradyrhizobium*. The circles from inside to outside in circus figure mean: *B. oligotrophicum* S58<sup>T</sup> *Nif* gene cluster, S58<sup>T</sup> GC%, *B. denitrificans* 80005, *B. oligotrophicum* LMG8443<sup>T</sup>, *B. oligotrophicum* 80025, *Bradyrhizobium* sp. II 80013, *Bradyrhizobium* sp. III 80001, *Bradyrhizobium* sp. IV 81033, *Bradyrhizobium* sp. V 80016, *Bradyrhizobium* sp. VII 82079, *Bradyrhizobium* sp. VIII 83002, *Bradyrhizobium* sp. VIII 83012, *Bradyrhizobium* sp. ORS 278, *Bradyrhizobium* sp. ORS 285, *Bradyrhizobium* sp. S23321, *B. betae* PL7HG1T, *Rhodopseudomonas palustris* BisA53, *Rhodopseudomonas palustris* BisB18.

The photosynthetic gene cluster in AIRs contains genes encoding bacterial chlorophylls, carotenoids, and photoreaction centers. There were also significant differences in the distribution and arrangement of these genes in different strains, indicating events of acquisition and loss of these genes in different evolutionary pathways. In particular, strains such as *Bradyrhizobium* sp. II 80013 may have acquired photosynthetic genes earlier in their evolutionary history and accumulated a large amount of genetic variation during subsequent evolution. In addition, the transmission of photosynthetic genes in AIRs is mainly vertical, which is similar to the mode of transmission of *nif* genes.

### 3.6. Analysis of T3SS Components

A widespread feature in rhizobia is the presence of T3SS, which consists of a core component (rhizobium conserved, *rhc*) and effector proteins (*Nops*). These effector proteins, secreted by the T3SS, play a crucial role in modulating the extent of rhizobial nodulation. Analysis of the composition of 11 genes encoding T3SS in *Bradyrhizobium* (Figure 10) revealed that the genes responsible for encoding the T3SS structure were commonly found across the *Bradyrhizobium* strains. Among the non-AIR strains, all 11 components were almost completely present. In contrast, among the 24 AIRs, only 9 strains had the complete set of genes encoding the T3SS structure, while the remaining strains primarily lacked the *rhcC1*, *rhcL*, and *rhcS* genes. In addition to the genomes of non-symbiotic *Bradyrhizobium*, the *rhcC1*, *rhcL*, and *rhcS* genes were also commonly absent. Furthermore, the *rhcT* gene was frequently missing as well. The similarity between the T3SS structure-encoding genes of AIRs and the reference strains displayed substantial variation. Sequence similarity ranged between 70% and 100% when comparing the T3SS structure-encoding genes of the reference strains with those in the T3SS database. Among the AIRs, *Bradyrhizobium* sp. DOA9 (CI-I type) and *Bradyrhizobium* ORS285 (CI-II type) exhibited high sequence similarity in the T3SS genes, which is consistent with previous research [74]. However, the similarities among the other strains were generally below 30%. The observed differences between the T3SS of AIRs and the reference strains suggest that there are structural variations in T3SS among them (Figure 10).

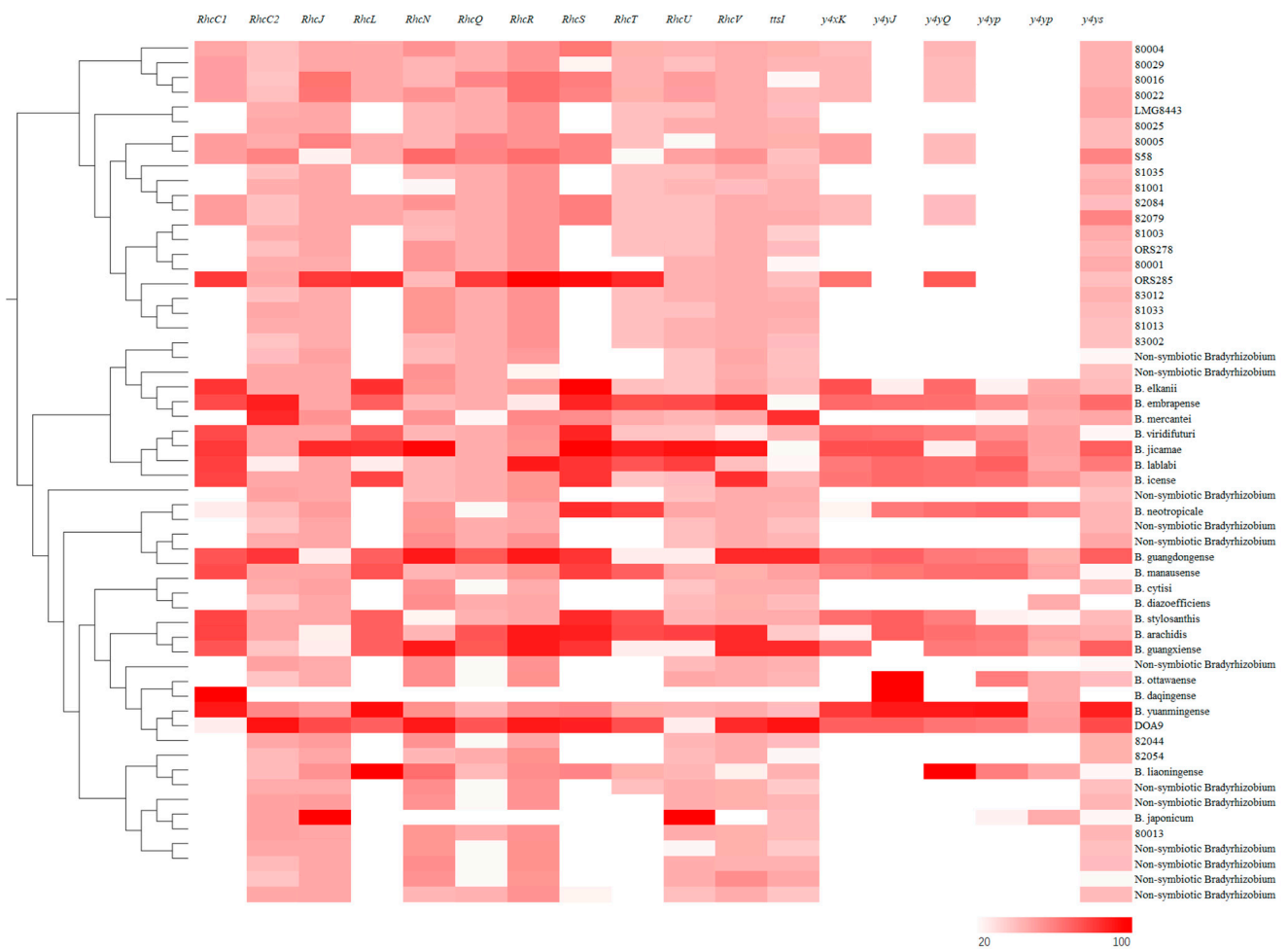


Figure 10. Analysis of T3SS components of *Bradyrhizobium*.

T3SS plays a crucial role in modulating the physiological state of plants through the secretion of effector proteins, which subsequently impact the extent of nodulation. This study also performed an analysis of 23 effector proteins in *Bradyrhizobium* (Figure 11), and the findings imply that in contrast to the T3SS structural genes, the effector proteins displayed substantial variation across different *Bradyrhizobium* taxa. The genome of non-AIRs contains numerous genes encoding effector proteins, and the repertoire of these proteins differs between strains. These variations in effector proteins are an important contributing factor to the host-specific differences observed among the strains. The lower levels of effector proteins in non-symbiotic *Bradyrhizobium* are related to its lifestyle. The genomes of *Bradyrhizobium* sp. DOA9 and *Bradyrhizobium* sp. ORS285 had a high number of effector proteins, while the rest of the genomes of *Bradyrhizobium* species had a low number of genes encoding effector proteins, and *nopM*, *nopU*, *nopV*, and *nopY* genes were present in the genomes of some strains. Albin experimented with the *ernA* gene mutant of *Bradyrhizobium* sp. ORS3257 (whose original host is cowpea) on nodulation with AIRs, and the mutant lost its ability to nodulate, indicating that the effector protein encoded by the *ernA* gene is important for the nodulation of AIRs [22]. We discovered that only the genome of *Bradyrhizobium* sp. ORS285 contained the *ernA* gene in AIRs. Additionally, a homolog of *ernA* was also found in the DOA9 genome, which is known to have a high number of effector proteins. However, no homolog of *ernA* was identified in the Indian AIRs. These findings suggest that the *ernA* gene plays a crucial role in the nodulation process of CI-I and CI-II types of AIRs but has little influence on the nodulation of CI-III type (Figure 11).

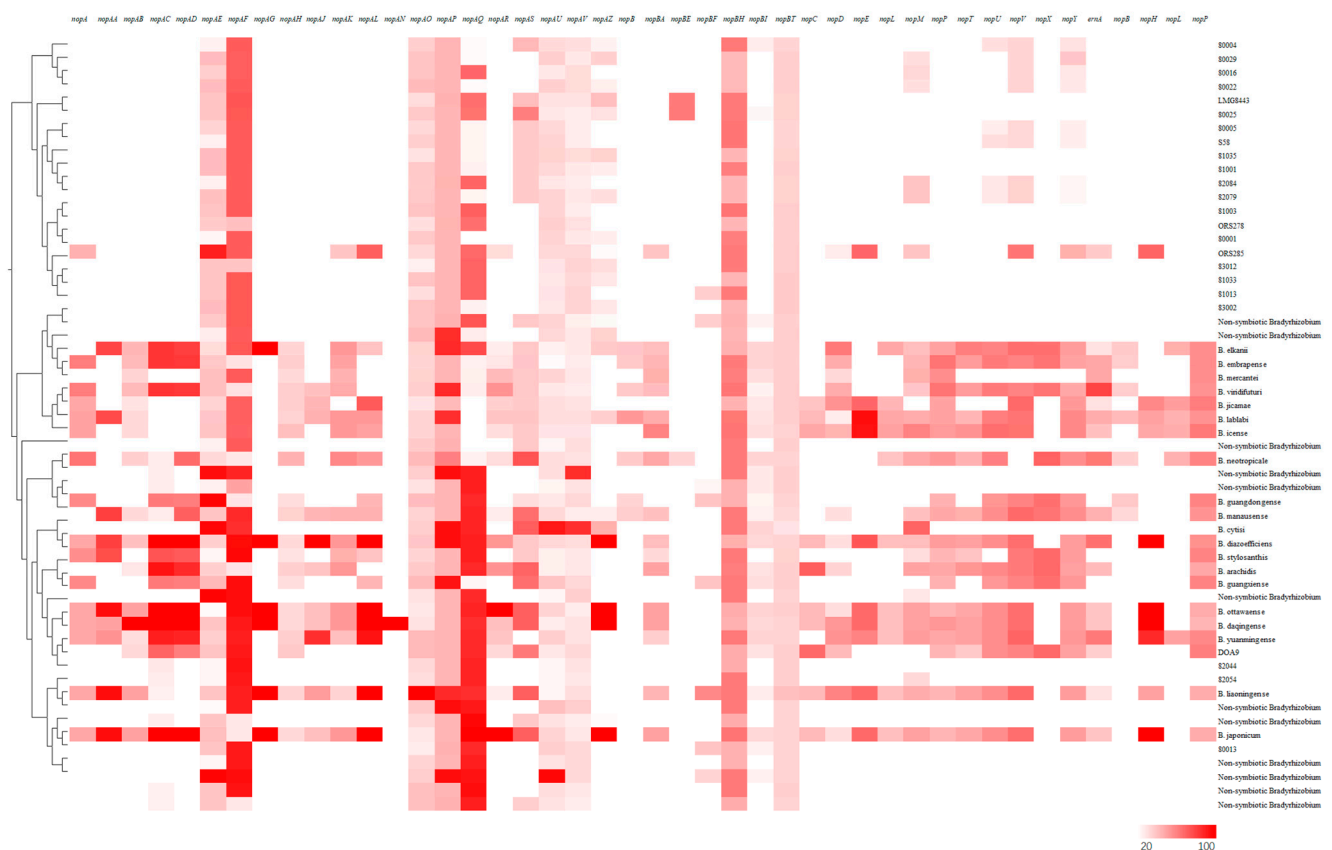


Figure 11. T3SS effecting factor analysis of *Bradyrhizobium*.

Recent studies have shown that the role of T3SS in symbiosis goes beyond the regulation of plant immune responses [75] and plays an important role in the NF-independent nodulation mode [74]. *Bradyrhizobium elkanii* USDA61 can nodulate symbiotically with soybean *nfr* mutants (which do not have the sensing ability of nodulation factor), whereas T3SS mutants cannot nodulate with them. Transcriptional analysis revealed increased

expression of the soybean nodulation-specific genes ENOD40 and NIN in roots of soybean plants inoculated with *B. elkanii* but not with the T3SS mutant, suggesting that T3SS activates the host nodulation signaling pathway by bypassing NF recognition [76]. T3SS structure does not appear to be a major influence on NF-independent nodal patterns, with *Bradyrhizobium* sp. ORS278 and BTAi1 able to nodulate with *Aeschynomene indica* in the absence of T3SS [19].

### 3.7. Analysis of the Genetic Evolution of *Bradyrhizobium*

Prokaryotic genomes are highly flexible, accompanied by the acquisition and loss of a large number of gene families in their evolutionary history [77]. To gain insight into the changes in the composition and content of gene families in the evolutionary history of AIRs, this study analyzed AIRs and reference strains of *Bradyrhizobium* and counted the gains and losses of gene families at different nodes in the species tree.

The results (Figure 12, Table S2) indicate that the evolutionary history of *Bradyrhizobium* was characterized by significant gene acquisition events. Analysis of the species tree and gene gains and losses revealed that the common ancestor genome of *Bradyrhizobium* initially possessed 3692 gene families. Subsequently, one lineage acquired 1072 gene families, leading to the evolution of the ancestor of AIRs. Another lineage acquired 310 gene families, resulting in the diversification of *Bradyrhizobium* and the emergence of non-symbiotic *Bradyrhizobium* strains. These findings highlight the importance of gene acquisition events in shaping the adaptive evolution of *Bradyrhizobium*. In Cluster I of the species tree, *Bradyrhizobium* sp. VII 81001 experienced a substantial loss of gene families during the species formation phase. A total of 1190 gene families were lost, which is the highest number observed among the 56 *Bradyrhizobium* strains. This loss of gene families also resulted in a significantly smaller genome size of 6.1 M compared to other strains. On the other hand, all *Bradyrhizobium* strains in Cluster II were found to be symbiotic, and no significant gene family losses were observed in this cluster. This suggests that *Bradyrhizobium* strains in Cluster II have been actively acquiring new gene families throughout their evolutionary history to adapt to different host selections. Cluster III of the species tree branch consists of a diverse group of *Bradyrhizobium* strains, including non-AIRs (such as *B. gunagxiense*, *B. ottawaense*, etc.), non-symbiotic *Bradyrhizobium* (e.g., *B. betae*, *Bradyrhizobium* sp. S23321, etc.), and AIRs (e.g., *Bradyrhizobium* sp. I, *Bradyrhizobium* sp. II, etc.). Similar to Cluster II, non-AIR strains have a history characterized by the acquisition of new gene families. Additionally, the presence of gene family losses in the evolutionary history of AIRs suggests that these host plants have selective preferences for certain rhizobial genomes. Consequently, *Bradyrhizobium* strains must undergo the loss of some functional genes to establish symbiosis with *A. indica*. This observation aligns with the absence of genes encoding nodulation factors in AIRs (Figure 12).

Gene loss can enable bacteria to adapt to specific niches [78]. For example, the loss of unnecessary metabolic genes can reduce energy consumption [79], thereby improving environmental adaptability and competitiveness. The newly obtained genes may give bacteria new functions [80], such as improving the ability to adapt to host plants. Throughout the whole evolution process, the loss of the gene family of AIRs was the most obvious, which indicated that *Bradyrhizobium* continuously lost genes during the symbiosis with AIRs, thus adapting and colonizing the host rhizosphere. In addition, the proportion of acquired and lost gene families during the evolution of *Bradyrhizobium* varies at different nodes, which may be related to the ecological environment and biological characteristics of different species.

### 3.8. Analysis of Differential Genes in *Bradyrhizobium*

The considerable phylogenetic distance observed between AIRs and the reference *Bradyrhizobium* strains (non-AIRs and non-symbiotic *Bradyrhizobium*), along with the patterns of gene acquisition and loss, strongly suggest that the genomes of both types of rhizobia have undergone extensive changes throughout their evolutionary history



enriched in AIRs were associated with bacterial invasion of epithelial cells, plant-pathogen interactions, Nod-like receptor signaling pathways, protein transport, photosynthesis, and carotenoid synthesis. These findings align with the trait of AIRs being photosynthetic [1,3,4,7,81] and adopting fissure infection [7]. The presence of the Nod-like receptor signaling pathway in AIRs suggests the existence of a system for sensing plant secretions, similar to NF-dependent types of rhizobia. On the other hand, the enrichment of metabolic pathways in the reference strains of *Bradyrhizobium* indicated the presence of pathways related to bacterial secretion systems, biofilm synthesis, and group-sensing responses. Additionally, this group of strains exhibited a high enrichment of disease-associated pathways, which could potentially be attributed to HGT events between non-symbiotic *Bradyrhizobium* and pathogenic bacteria present in the environment. This transfer might have resulted in the acquisition of accessory genes associated with disease pathways. Alternatively, it is possible that certain genes within *Bradyrhizobia* have functional similarities to proteins or enzymes involved in these disease pathways (Table 2).

**Table 2.** Enrichment and analysis of homologous gene family difference gene KEGG in *Aeschynomene indica* rhizobia and reference strain.

Taxa	Number of Homologous Gene Families with Differences	Number of KEGG Pathways	Number of Exclusive Access Points	Typical Pathways
<i>Aeschynomene indica</i> rhizobia	1877	159	16	Bacterial infestation of epithelial cells, carotenoid synthesis, Nod-like receptor signaling pathway, O-glycan biosynthesis, photosynthesis, plant-pathogen interactions, protein transport, etc.
Reference strains	5211	221	68	Bacterial secretion systems, biofilm synthesis, swarm-sensing effects, etc.

Specifically, genes involved in carotenoid synthesis encode phytoene synthase, phytoene desaturase, lycopene- $\beta$ -cyclase, and  $\epsilon$ -ring hydroxylase [82]. Phytoene synthase catalyzes the first committed step in the carotenoid biosynthesis pathway and is a major rate-limiting enzyme of carotenogenesis [83]. Phytoene desaturase and  $\epsilon$ -ring hydroxylase are essential plant carotenoid biosynthetic enzymes [84,85]. Lycopene- $\beta$ -cyclases are key enzymes located at the branch point of the carotenoid biosynthesis pathway [86]. The functions of these proteins may be related to the photosynthetic ability of AIRs.

#### 4. Conclusions

The NF-independent nodulation mechanism of *A. indica* currently lacks a universally accepted explanation; in this study, a comprehensive analysis of the acquisition and loss of gene families of AIRs and reference strains, followed by KEGG annotation of the gene families specific to AIRs, was performed. The findings revealed that AIRs have three distinct origins: early AIRs, non-symbiotic *Bradyrhizobium*, and non-AIRs. The phylogenetic tree of the *nif* gene cluster in AIRs exhibited a high degree of concordance with the housekeeping genes, suggesting that significant HGT events have not occurred. Furthermore, the GC content of several regions in the AIR genome was significantly lower than the average GC content of the genome, indicating the occurrence of HGT. A comparative analysis of the genomes of AIRs and the reference strains of *Bradyrhizobium* revealed that AIRs generally lack nodulation genes, while the abundance of type III secretion system effectors in their genome is lower. However, a great conservation level was observed in *nif* genes and photosynthesis genes. Most of the genes specific to the genome of AIRs are associated with

pathogen infestation. These genes may play a role in the NF-independent nodulation mode observed in AIRs. The KEGG analysis showed that genes specific to AIRs are enriched in epithelial cell invasion, carotenoid synthesis, nod-like receptor signaling pathway, O-glycan biosynthesis, photosynthesis, plant-pathogen interactions, protein transport, and other pathways. However, the elucidation of the NF-independent nodulation mechanism requires further investigation.

**Supplementary Materials:** The following supporting information can be downloaded at: <https://www.mdpi.com/article/10.3390/agronomy14061295/s1>, Table S1: The genome used in comparative genomic analysis of *A. indica Bradyrhizobium*; Table S2: The gains and losses of gene families of different nodes; Table S3: Enrichment and analysis of homologous gene family difference gene KEGG in *A. indica Bradyrhizobium* and reference strain.

**Author Contributions:** M.Z.: Data Curation, Writing—original draft. J.D.: Data Curation, Formal Analysis. Z.Z.: Data Curation, Formal Analysis, Methodology, Visualization. E.W.: Writing—Review and Editing. H.X.: Visualization. C.W.: Writing—Review and Editing. D.W.: Writing—Review and Editing. Z.X.: Data curation, Supervision, Project Administration, Funding Acquisition, Writing—Review and Editing. All authors have read and agreed to the published version of the manuscript.

**Funding:** This work was supported by the Shandong Key Research and Development Program (2021CXGC010804) and the National Natural Science Foundation of China (32270065).

**Data Availability Statement:** The original contributions presented in the study are included in the article, further inquiries can be directed to the corresponding author.

**Acknowledgments:** We thank Yan Li for his valuable suggestions.

**Conflicts of Interest:** The authors declare no conflicts of interest.

## References

- Zhang, Z.; Li, Y.; Pan, X.; Shao, S.; Liu, W.; Wang, E.T.; Xie, Z. *Aeschynomene indica*-Nodulating Rhizobia Lacking Nod Factor Synthesis Genes: Diversity and Evolution in Shandong Peninsula, China. *Appl. Environ. Microbiol.* **2019**, *85*, e00782-19. [[CrossRef](#)]
- Boivin, C.; Ndoye, I.; Molouba, F.; de Lajudie, P.; Dupuy, N.; Dreyfus, B.; de Bruijn, F.J. Stem Nodulation in Legumes: Diversity, Mechanisms, and Unusual Characteristics. *Crit. Rev. Plant Sci.* **1997**, *16*, 1–30. [[CrossRef](#)]
- Miche, L.; Moulin, L.; Chaintreuil, C.; Contreras-Jimenez, J.L.; Munive-Hernandez, J.A.; Del Carmen Villegas-Hernandez, M.; Crozier, F.; Bena, G. Diversity analyses of *Aeschynomene* symbionts in Tropical Africa and Central America reveal that nod-independent stem nodulation is not restricted to photosynthetic bradyrhizobia. *Environ. Microbiol.* **2010**, *12*, 2152–2164. [[CrossRef](#)]
- Molouba, F.; Lorquin, J.; Willems, A.; Hoste, B.; Giraud, E.; Dreyfus, B.; Gillis, M.; de Lajudie, P.; Masson-Boivin, C. Photosynthetic bradyrhizobia from *Aeschynomene* spp. are specific to stem-nodulated species and form a separate 16S ribosomal DNA restriction fragment length polymorphism group. *Appl. Environ. Microbiol.* **1999**, *65*, 3084–3094. [[CrossRef](#)] [[PubMed](#)]
- Mornico, D.; Miché, L.; Béna, G.; Nouwen, N.; Verméglia, A.; Vallenet, D.; Smith, A.A.; Giraud, E.; Médigue, C.; Moulin, L. Comparative genomics of *Aeschynomene* symbionts: Insights into the ecological lifestyle of nod-independent photosynthetic bradyrhizobia. *Genes* **2011**, *3*, 35–61. [[CrossRef](#)] [[PubMed](#)]
- Avontuur, J.R.; Palmer, M.; Beukes, C.W.; Chan, W.Y.; Coetzee, M.P.A.; Blom, J.; Stepkowski, T.; Kyrpides, N.C.; Woyke, T.; Shapiro, N.; et al. Genome-informed *Bradyrhizobium* taxonomy: Where to from here? *Syst. Appl. Microbiol.* **2019**, *42*, 427–439. [[CrossRef](#)]
- Bonaldi, K.; Gargani, D.; Prin, Y.; Fardoux, J.; Gully, D.; Nouwen, N.; Goormachtig, S.; Giraud, E. Nodulation of *Aeschynomene afraspera* and *A. indica* by photosynthetic *Bradyrhizobium* Sp. strain ORS285: The nod-dependent versus the nod-independent symbiotic interaction. *Mol. Plant Microbe Interact.* **2011**, *24*, 1359–1371. [[CrossRef](#)]
- Chaintreuil, C.; Gully, D.; Hervouet, C.; Tittabutr, P.; Randriambanona, H.; Brown, S.C.; Lewis, G.P.; Bourge, M.; Cartieaux, F.; Boursot, M.; et al. The evolutionary dynamics of ancient and recent polyploidy in the African semiaquatic species of the legume genus *Aeschynomene*. *New Phytol.* **2016**, *211*, 1077–1091. [[CrossRef](#)] [[PubMed](#)]
- Avontuur, J.R.; Wilken, P.M.; Palmer, M.; Coetzee, M.P.A.; Stepkowski, T.; Venter, S.N.; Steenkamp, E.T. Complex evolutionary history of photosynthesis in *Bradyrhizobium*. *Microb. Genom.* **2023**, *9*, 001105. [[CrossRef](#)]
- Wettlaufer, S.H.; Hardy, R.W. Effect of Light and Organic Acids on Oxygen Uptake by BTAi 1, a Photosynthetic Rhizobium. *Appl. Environ. Microbiol.* **1992**, *58*, 3830–3833. [[CrossRef](#)]
- Evans, W.R.; Fleischman, D.E.; Calvert, H.E.; Pyati, P.V.; Alter, G.M.; Rao, N.S. Bacteriochlorophyll and Photosynthetic Reaction Centers in Rhizobium Strain BTAi 1. *Appl. Environ. Microbiol.* **1990**, *56*, 3445–3449. [[CrossRef](#)] [[PubMed](#)]

12. Okubo, T.; Fukushima, S.; Itakura, M.; Oshima, K.; Longtonglang, A.; Teaumroong, N.; Mitsui, H.; Hattori, M.; Hattori, R.; Hattori, T.; et al. Genome analysis suggests that the soil oligotrophic bacterium *Agromonas oligotrophica* (*Bradyrhizobium oligotrophicum*) is a nitrogen-fixing symbiont of *Aeschynomene indica*. *Appl. Environ. Microbiol.* **2013**, *79*, 2542–2551. [[CrossRef](#)] [[PubMed](#)]
13. Yurkov, V.; Beatty, J.T. Isolation of aerobic anoxygenic photosynthetic bacteria from black smoker plume waters of the Juan de Fuca ridge in the Pacific Ocean. *Appl. Environ. Microbiol.* **1998**, *64*, 337–341. [[CrossRef](#)] [[PubMed](#)]
14. Knaff, D.B. Anoxygenic photosynthetic bacteria. *Photosynth. Res.* **1996**, *47*, 199–200. [[CrossRef](#)]
15. Jaubert, M.; Vuillet, L.; Hannibal, L.; Adriano, J.M.; Fardoux, J.; Bouyer, P.; Bonaldi, K.; Fleischman, D.; Giraud, E.; Verméglio, A. Control of peripheral light-harvesting complex synthesis by a bacteriophytochrome in the aerobic photosynthetic bacterium *Bradyrhizobium* strain BTAi1. *J. Bacteriol.* **2008**, *190*, 5824–5831. [[CrossRef](#)] [[PubMed](#)]
16. Giraud, E.; Hannibal, L.; Fardoux, J.; Verméglio, A.; Dreyfus, B. Effect of *Bradyrhizobium* photosynthesis on stem nodulation of *Aeschynomene sensitiva*. *Proc. Natl. Acad. Sci. USA* **2000**, *97*, 14795–14800. [[CrossRef](#)]
17. Tank, M.; Thiel, V.; Imhoff, J.F. Phylogenetic relationship of phototrophic purple sulfur bacteria according to pufL and pufM genes. *Int. Microbiol.* **2009**, *12*, 175–185.
18. Chen, W.F.; Wang, E.T.; Ji, Z.J.; Zhang, J.J. Recent development and new insight of diversification and symbiosis specificity of legume rhizobia: Mechanism and application. *J. Appl. Microbiol.* **2021**, *131*, 553–563. [[CrossRef](#)]
19. Giraud, E.; Moulin, L.; Vallenet, D.; Barbe, V.; Cytryn, E.; Avarre, J.C.; Jaubert, M.; Simon, D.; Cartieaux, F.; Prin, Y.; et al. Legume symbioses: Absence of Nod genes in photosynthetic bradyrhizobia. *Science* **2007**, *316*, 1307–1312. [[CrossRef](#)]
20. Guha, S.; Molla, F.; Sarkar, M.; Ibañez, F.; Fabra, A.; DasGupta, M. Nod factor-independent ‘crack-entry’ symbiosis in dalbergoid legume *Arachis hypogaea*. *Environ. Microbiol.* **2022**, *24*, 2732–2746. [[CrossRef](#)]
21. Busset, N.; Di Lorenzo, F.; Palmigiano, A.; Sturiale, L.; Gressent, F.; Fardoux, J.; Gully, D.; Chaintreuil, C.; Molinaro, A.; Silipo, A.; et al. The Very Long Chain Fatty Acid (C<sub>26</sub>:25OH) Linked to the Lipid A Is Important for the Fitness of the Photosynthetic *Bradyrhizobium* Strain ORS278 and the Establishment of a Successful Symbiosis with *Aeschynomene* Legumes. *Front. Microbiol.* **2017**, *8*, 1821. [[CrossRef](#)]
22. Teulet, A.; Busset, N.; Fardoux, J.; Gully, D.; Chaintreuil, C.; Cartieaux, F.; Jauneau, A.; Comorge, V.; Okazaki, S.; Kaneko, T.; et al. The rhizobial type III effector ErnA confers the ability to form nodules in legumes. *Proc. Natl. Acad. Sci. USA* **2019**, *116*, 21758–21768. [[CrossRef](#)] [[PubMed](#)]
23. Teulet, A.; Gully, D.; Rouy, Z.; Camuel, A.; Koebnik, R.; Giraud, E.; Lassalle, F. Phylogenetic distribution and evolutionary dynamics of nod and T3SS genes in the genus *Bradyrhizobium*. *Microb. Genom.* **2020**, *6*, e000407. [[CrossRef](#)] [[PubMed](#)]
24. Camuel, A.; Teulet, A.; Carcagno, M.; Haq, F.; Pacquit, V.; Gully, D.; Pervent, M.; Chaintreuil, C.; Fardoux, J.; Horta-Araujo, N.; et al. Widespread *Bradyrhizobium* distribution of diverse Type III effectors that trigger legume nodulation in the absence of Nod factor. *ISME J.* **2023**, *17*, 1416–1429. [[CrossRef](#)] [[PubMed](#)]
25. Weston, L.A.; Mathesius, U. Flavonoids: Their structure, biosynthesis and role in the rhizosphere, including allelopathy. *J. Chem. Ecol.* **2013**, *39*, 283–297. [[CrossRef](#)] [[PubMed](#)]
26. Bosse, M.A.; Silva, M.B.D.; Oliveira, N.; Araujo, M.A.; Rodrigues, C.; Azevedo, J.P.; Reis, A.R.D. Physiological impact of flavonoids on nodulation and ureide metabolism in legume plants. *Plant Physiol. Biochem.* **2021**, *166*, 512–521. [[CrossRef](#)] [[PubMed](#)]
27. Wassem, R.; Kobayashi, H.; Kambara, K.; Le Quere, A.; Walker, G.C.; Broughton, W.J.; Deakin, W.J. TtsI regulates symbiotic genes in *Rhizobium* species NGR234 by binding to tts boxes. *Mol. Microbiol.* **2008**, *68*, 736–748. [[CrossRef](#)] [[PubMed](#)]
28. Pérez-Montaña, F.; Jiménez-Guerrero, I.; Acosta-Jurado, S.; Navarro-Gómez, P.; Ollero, F.J.; Ruiz-Sainz, J.E.; López-Baena, F.J.; Vinardell, J.M. A transcriptomic analysis of the effect of genistein on *Sinorhizobium fredii* HH103 reveals novel rhizobial genes putatively involved in symbiosis. *Sci. Rep.* **2016**, *6*, 31592. [[CrossRef](#)] [[PubMed](#)]
29. Arashida, H.; Odake, H.; Sugawara, M.; Noda, R.; Kakizaki, K.; Ohkubo, S.; Mitsui, H.; Sato, S.; Minamisawa, K. Evolution of rhizobial symbiosis islands through insertion sequence-mediated deletion and duplication. *ISME J.* **2022**, *16*, 112–121. [[CrossRef](#)]
30. Dagan, T.; Martin, W. Ancestral genome sizes specify the minimum rate of lateral gene transfer during prokaryote evolution. *Proc. Natl. Acad. Sci. USA* **2007**, *104*, 870–875. [[CrossRef](#)]
31. Arnold, B.J.; Huang, I.T.; Hanage, W.P. Horizontal gene transfer and adaptive evolution in bacteria. *Nat. Rev. Microbiol.* **2022**, *20*, 206–218. [[CrossRef](#)] [[PubMed](#)]
32. Liu, S.; Jiao, J.; Tian, C.F. Adaptive Evolution of Rhizobial Symbiosis beyond Horizontal Gene Transfer: From Genome Innovation to Regulation Reconstruction. *Genes* **2023**, *14*, 274. [[CrossRef](#)] [[PubMed](#)]
33. Prjibelski, A.; Antipov, D.; Meleshko, D.; Lapidus, A.; Korobeynikov, A. Using SPAdes De Novo Assembler. *Curr. Protoc. Bioinform.* **2020**, *70*, e102. [[CrossRef](#)] [[PubMed](#)]
34. Walker, B.J.; Abeel, T.; Shea, T.; Priest, M.; Abouelliel, A.; Sakthikumar, S.; Cuomo, C.A.; Zeng, Q.; Wortman, J.; Young, S.K.; et al. Pilon: An integrated tool for comprehensive microbial variant detection and genome assembly improvement. *PLoS ONE* **2014**, *9*, e112963. [[CrossRef](#)]
35. Du, Z.; Wu, Q.; Wang, T.; Chen, D.; Huang, X.; Yang, W.; Luo, W. BlastGUI: A Python-based Cross-platform Local BLAST Visualization Software. *Mol. Inform.* **2020**, *39*, e1900120. [[CrossRef](#)] [[PubMed](#)]
36. Emms, D.M.; Kelly, S. OrthoFinder: Phylogenetic orthology inference for comparative genomics. *Genome Biol.* **2019**, *20*, 238. [[CrossRef](#)]

37. Letunic, I.; Bork, P. Interactive Tree Of Life (iTOL) v5: An online tool for phylogenetic tree display and annotation. *Nucleic Acids Res.* **2021**, *49*, W293–W296. [[CrossRef](#)] [[PubMed](#)]
38. Hyatt, D.; Chen, G.L.; Locascio, P.F.; Land, M.L.; Larimer, F.W.; Hauser, L.J. Prodigal: Prokaryotic gene recognition and translation initiation site identification. *BMC Bioinform.* **2010**, *11*, 119. [[CrossRef](#)] [[PubMed](#)]
39. Buchfink, B.; Xie, C.; Huson, D.H. Fast and sensitive protein alignment using DIAMOND. *Nat. Methods* **2015**, *12*, 59–60. [[CrossRef](#)]
40. Reau, M.; Lagarde, N.; Zagury, J.F.; Montes, M. Nuclear Receptors Database Including Negative Data (NR-DBIND): A Database Dedicated to Nuclear Receptors Binding Data Including Negative Data and Pharmacological Profile. *J. Med. Chem.* **2019**, *62*, 2894–2904. [[CrossRef](#)]
41. Gasteiger, E.; Jung, E.; Bairoch, A. SWISS-PROT: Connecting biomolecular knowledge via a protein database. *Curr. Issues Mol. Biol.* **2001**, *3*, 47–55. [[CrossRef](#)] [[PubMed](#)]
42. Rasche, H.; Hiltmann, S. Galactic Circos: User-friendly Circos plots within the Galaxy platform. *Gigascience* **2020**, *9*, g1aa065. [[CrossRef](#)]
43. Kanehisa, M.; Furumichi, M.; Sato, Y.; Kawashima, M.; Ishiguro-Watanabe, M. KEGG for taxonomy-based analysis of pathways and genomes. *Nucleic Acids Res.* **2022**, *51*, D587–D592. [[CrossRef](#)] [[PubMed](#)]
44. Chauhan, A.; Rathore, R.S.; Agarwal, M.; Chauhan, A.J.; Taywade, A. Friend or Foe: Draft Genome Sequence of *Bradyrhizobium* sp. Strain SRS-191. *Microbiol. Resour. Announc.* **2022**, *11*, e0075322. [[CrossRef](#)]
45. Toniutti, M.A.; Albicoro, F.J.; Castellani, L.G.; Lopez Garcia, S.L.; Fornasero, L.V.; Zuber, N.E.; Vera, L.M.; Vacca, C.; Cafiero, J.H.; Winkler, A.; et al. Genome sequence of *Bradyrhizobium yuanmingense* strain P10 130, a highly efficient nitrogen-fixing bacterium that could be used for *Desmodium incanum* inoculation. *Gene* **2021**, *768*, 145267. [[CrossRef](#)]
46. Krishnan, H.B.; Kim, W.S.; Givan, S.A. Draft Genome Sequence of *Bradyrhizobium* sp. Strain LVM 105, a Nitrogen-Fixing Symbiont of *Chamaecrista fasciculata* (Michx.) Greene. *Microbiol. Resour. Announc.* **2019**, *8*, e00132-19. [[CrossRef](#)]
47. Bromfield, E.S.P.; Cloutier, S.; Nguyen, H.D.T. Description and complete genome sequences of *Bradyrhizobium symbiodeficiens* sp. nov., a non-symbiotic bacterium associated with legumes native to Canada. *Int. J. Syst. Evol. Microbiol.* **2020**, *70*, 442–449. [[CrossRef](#)] [[PubMed](#)]
48. Sun, L.; Zhang, Z.; Dong, X.; Tang, Z.; Ju, B.; Du, Z.; Wang, E.; Xie, Z. *Bradyrhizobium aescynomenes* sp. nov., a root and stem nodule microsymbiont of *Aeschynomene indica*. *Syst. Appl. Microbiol.* **2022**, *45*, 126337. [[CrossRef](#)] [[PubMed](#)]
49. Rejili, M.; Off, K.; Brachmann, A.; Marin, M. *Bradyrhizobium hipponense* sp. nov., isolated from *Lupinus angustifolius* growing in the northern region of Tunisia. *Int. J. Syst. Evol. Microbiol.* **2020**, *70*, 5539–5550. [[CrossRef](#)]
50. Simoes-Araujo, J.L.; Leite, J.; Passos, S.R.; Xavier, G.R.; Rumjanek, N.G.; Zilli, J.E. Draft genome sequence of *Bradyrhizobium* sp. strain BR 3267, an elite strain recommended for cowpea inoculation in Brazil. *Braz. J. Microbiol.* **2016**, *47*, 781–782. [[CrossRef](#)]
51. Zhang, N.; Jin, C.Z.; Zhuo, Y.; Li, T.; Jin, F.J.; Lee, H.G.; Jin, L. Genetic diversity into a novel free-living species of *Bradyrhizobium* from contaminated freshwater sediment. *Front. Microbiol.* **2023**, *14*, 1295854. [[CrossRef](#)] [[PubMed](#)]
52. Tomkins, J.P.; Wood, T.C.; Stacey, M.G.; Loh, J.T.; Judd, A.; Goicoechea, J.L.; Stacey, G.; Sadowsky, M.J.; Wing, R.A. A marker-dense physical map of the *Bradyrhizobium japonicum* genome. *Genome Res.* **2001**, *11*, 1434–1440. [[CrossRef](#)] [[PubMed](#)]
53. Blommaert, J. Genome size evolution: Towards new model systems for old questions. *Proc. Biol. Sci.* **2020**, *287*, 20201441. [[CrossRef](#)] [[PubMed](#)]
54. Nouwen, N.; Chaintreuil, C.; Fardoux, J.; Giraud, E. A glutamate synthase mutant of *Bradyrhizobium* sp. strain ORS285 is unable to induce nodules on Nod factor-independent *Aeschynomene* species. *Sci. Rep.* **2021**, *11*, 20910. [[CrossRef](#)] [[PubMed](#)]
55. Stepkowski, T.; Watkin, E.; McInnes, A.; Gurda, D.; Gracz, J.; Steenkamp, E.T. Distinct *Bradyrhizobium* communities nodulate legumes native to temperate and tropical monsoon Australia. *Mol. Phylogenet. Evol.* **2012**, *63*, 265–277. [[CrossRef](#)] [[PubMed](#)]
56. Sprent, J.I.; Ardley, J.; James, E.K. Biogeography of nodulated legumes and their nitrogen-fixing symbionts. *New Phytol.* **2017**, *215*, 40–56. [[CrossRef](#)] [[PubMed](#)]
57. Beukes, C.W.; Stepkowski, T.; Venter, S.N.; Clapa, T.; Phalane, F.L.; le Roux, M.M.; Steenkamp, E.T. Crotonariaeae and Genisteeae of the South African Great Escarpment are nodulated by novel *Bradyrhizobium* species with unique and diverse symbiotic loci. *Mol. Phylogenet. Evol.* **2016**, *100*, 206–218. [[CrossRef](#)] [[PubMed](#)]
58. Cloutier, S.; Bromfield, E.S.P. Analysis of the Complete Genome Sequence of the Widely Studied Strain *Bradyrhizobium betae* PL7HG1(T) Reveals the Presence of Photosynthesis Genes and a Putative Plasmid. *Microbiol. Resour. Announc.* **2019**, *8*, 01282-19. [[CrossRef](#)] [[PubMed](#)]
59. Brown, S.D.; Utturkar, S.M.; Klingeman, D.M.; Johnson, C.M.; Martin, S.L.; Land, M.L.; Lu, T.Y.; Schadt, C.W.; Doktycz, M.J.; Pelletier, D.A. Twenty-one genome sequences from *Pseudomonas* species and 19 genome sequences from diverse bacteria isolated from the rhizosphere and endosphere of *Populus deltoides*. *J. Bacteriol.* **2012**, *194*, 5991–5993. [[CrossRef](#)]
60. Fabra, A.; Castro, S.; Taurian, T.; Angelini, J.; Ibañez, F.; Dardanelli, M.; Tonelli, M.; Bianucci, E.; Valetti, L. Interaction among *Arachis hypogaea* L. (peanut) and beneficial soil microorganisms: How much is it known? *Crit. Rev. Microbiol.* **2010**, *36*, 179–194. [[CrossRef](#)]
61. Stecher, B.; Maier, L.; Hardt, W.D. ‘Blooming’ in the gut: How dysbiosis might contribute to pathogen evolution. *Nat. Rev. Microbiol.* **2013**, *11*, 277–284. [[CrossRef](#)]
62. Doucet-Populaire, F.; Trieu-Cuot, P.; Dosbaa, I.; Andremont, A.; Courvalin, P. Inducible transfer of conjugative transposon Tn1545 from *Enterococcus faecalis* to *Listeria monocytogenes* in the digestive tracts of gnotobiotic mice. *Antimicrob. Agents Chemother.* **1991**, *35*, 185–187. [[CrossRef](#)]

63. Sun, J.; Qiu, Y.; Ding, P.; Peng, P.; Yang, H.; Li, L. Conjugative Transfer of Dioxin-Catabolic Megaplastids and Bioaugmentation Prospects of a *Rhodococcus* sp. *Environ. Sci. Technol.* **2017**, *51*, 6298–6307. [[CrossRef](#)]
64. Kim, M.K.; Ha, H.S.; Choi, S.U. Conjugal transfer using the bacteriophage phiC31 att/int system and properties of the attB site in *Streptomyces ambifaciens*. *Biotechnol. Lett.* **2008**, *30*, 695–699. [[CrossRef](#)] [[PubMed](#)]
65. Hulin, M.T.; Rabiey, M.; Zeng, Z.; Vadillo Dieguez, A.; Bellamy, S.; Swift, P.; Mansfield, J.W.; Jackson, R.W.; Harrison, R.J. Genomic and functional analysis of phage-mediated horizontal gene transfer in *Pseudomonas syringae* on the plant surface. *New Phytol.* **2023**, *237*, 959–973. [[CrossRef](#)]
66. González-Villalobos, E.; Balcázar, J.L. Does phage-mediated horizontal gene transfer represent an environmental risk? *Trends Microbiol.* **2022**, *30*, 1022–1024. [[CrossRef](#)]
67. Kenzaka, T.; Tani, K.; Nasu, M. High-frequency phage-mediated gene transfer in freshwater environments determined at single-cell level. *ISME J.* **2010**, *4*, 648–659. [[CrossRef](#)] [[PubMed](#)]
68. Baev, N.; Schultze, M.; Barlier, I.; Ha, D.C.; Virelizier, H.; Kondorosi, E.; Kondorosi, A. Rhizobium nodM and nodN genes are common nod genes: nodM encodes functions for efficiency of nod signal production and bacteroid maturation. *J. Bacteriol.* **1992**, *174*, 7555–7565. [[CrossRef](#)] [[PubMed](#)]
69. Yan, H.; Xie, J.B.; Ji, Z.J.; Yuan, N.; Tian, C.F.; Ji, S.K.; Wu, Z.Y.; Zhong, L.; Chen, W.X.; Du, Z.L.; et al. Evolutionarily Conserved nodE, nodO, T1SS, and Hydrogenase System in Rhizobia of *Astragalus membranaceus* and *Caragana intermedia*. *Front. Microbiol.* **2017**, *8*, 2282. [[CrossRef](#)]
70. Ke, X.; Xiao, H.; Peng, Y.; Wang, J.; Lv, Q.; Wang, X. Phosphoenolpyruvate reallocation links nitrogen fixation rates to root nodule energy state. *Science* **2022**, *378*, 971–977. [[CrossRef](#)]
71. Lindström, K.; Mousavi, S.A. Effectiveness of nitrogen fixation in rhizobia. *Microb. Biotechnol.* **2020**, *13*, 1314–1335. [[CrossRef](#)]
72. Okubo, T.; Tsukui, T.; Maita, H.; Okamoto, S.; Oshima, K.; Fujisawa, T.; Saito, A.; Futamata, H.; Hattori, R.; Shimomura, Y.; et al. Complete genome sequence of *Bradyrhizobium* sp. S23321: Insights into symbiosis evolution in soil oligotrophs. *Microbes Environ.* **2012**, *27*, 306–315. [[CrossRef](#)]
73. Sun, T.; Wang, P.; Rao, S.; Zhou, X.; Wrightstone, E.; Lu, S.; Yuan, H.; Yang, Y.; Fish, T.; Thannhauser, T.; et al. Co-chaperoning of chlorophyll and carotenoid biosynthesis by ORANGE family proteins in plants. *Mol. Plant* **2023**, *16*, 1048–1065. [[CrossRef](#)]
74. Okazaki, S.; Tittabutr, P.; Teulet, A.; Thouin, J.; Fardoux, J.; Chaintreuil, C.; Gully, D.; Arrighi, J.F.; Furuta, N.; Miwa, H.; et al. Rhizobium-legume symbiosis in the absence of Nod factors: Two possible scenarios with or without the T3SS. *ISME J.* **2016**, *10*, 64–74. [[CrossRef](#)]
75. Teulet, A.; Camuel, A.; Perret, X.; Giraud, E. The Versatile Roles of Type III Secretion Systems in Rhizobium-Legume Symbioses. *Annu. Rev. Microbiol.* **2022**, *76*, 45–65. [[CrossRef](#)]
76. Okazaki, S.; Kaneko, T.; Sato, S.; Saeki, K. Hijacking of leguminous nodulation signaling by the rhizobial type III secretion system. *Proc. Natl. Acad. Sci. USA* **2013**, *110*, 17131–17136. [[CrossRef](#)]
77. Periwal, V.; Scaria, V. Insights into structural variations and genome rearrangements in prokaryotic genomes. *Bioinformatics* **2015**, *31*, 1–9. [[CrossRef](#)]
78. Polz, M.F.; Alm, E.J.; Hanage, W.P. Horizontal gene transfer and the evolution of bacterial and archaeal population structure. *Trends Genet.* **2013**, *29*, 170–175. [[CrossRef](#)]
79. Kelly, S. The economics of organellar gene loss and endosymbiotic gene transfer. *Genome Biol.* **2021**, *22*, 345. [[CrossRef](#)] [[PubMed](#)]
80. de Mattos, K.; Viger, R.S.; Tremblay, J.J. Transcription Factors in the Regulation of Leydig Cell Gene Expression and Function. *Front. Endocrinol.* **2022**, *13*, 881309. [[CrossRef](#)] [[PubMed](#)]
81. Chaintreuil, C.; Perrier, X.; Martin, G.; Fardoux, J.; Lewis, G.P.; Brottier, L.; Rivallan, R.; Gomez-Pacheco, M.; Bourges, M.; Lamy, L.; et al. Naturally occurring variations in the nod-independent model legume *Aeschynomene evenia* and relatives: A resource for nodulation genetics. *BMC Plant Biol.* **2018**, *18*, 54. [[CrossRef](#)] [[PubMed](#)]
82. Schüler, L.M.; Bombo, G.; Duarte, P.; Santos, T.F.; Maia, I.B.; Pinheiro, F.; Marques, J.; Jacinto, R.; Schulze, P.S.C.; Pereira, H.; et al. Carotenoid biosynthetic gene expression, pigment and n-3 fatty acid contents in carotenoid-rich *Tetraselmis striata* CTP4 strains under heat stress combined with high light. *Bioresour. Technol.* **2021**, *337*, 125385. [[CrossRef](#)] [[PubMed](#)]
83. Zhou, X.; Rao, S.; Wrightstone, E.; Sun, T.; Lui, A.C.W.; Welsch, R.; Li, L. Phytoene Synthase: The Key Rate-Limiting Enzyme of Carotenoid Biosynthesis in Plants. *Front. Plant Sci.* **2022**, *13*, 884720. [[CrossRef](#)] [[PubMed](#)]
84. Koschmieder, J.; Fehling-Kaschek, M.; Schaub, P.; Ghisla, S.; Brausemann, A.; Timmer, J.; Beyer, P. Plant-type phytoene desaturase: Functional evaluation of structural implications. *PLoS ONE* **2017**, *12*, e0187628. [[CrossRef](#)] [[PubMed](#)]
85. Wang, S.; Zhuang, K.; Zhang, S.; Yang, M.; Kong, F.; Meng, Q. Overexpression of a tomato carotenoid  $\epsilon$ -hydroxylase gene (SILUT1) improved the drought tolerance of transgenic tobacco. *J. Plant Physiol.* **2018**, *222*, 103–112. [[CrossRef](#)]
86. Lu, S.; Zhang, Y.; Zheng, X.; Zhu, K.; Xu, Q.; Deng, X. Isolation and Functional Characterization of a Lycopene  $\beta$ -cyclase Gene Promoter from Citrus. *Front. Plant Sci.* **2016**, *7*, 1367. [[CrossRef](#)]

**Disclaimer/Publisher’s Note:** The statements, opinions and data contained in all publications are solely those of the individual author(s) and contributor(s) and not of MDPI and/or the editor(s). MDPI and/or the editor(s) disclaim responsibility for any injury to people or property resulting from any ideas, methods, instructions or products referred to in the content.